

# The Size of Local Bispectrum and Trispectrum in a Non-Minimal Inflation

Kosar Asadi\* and Kouros Nozari†

*Department of Physics, Faculty of Basic Sciences,  
University of Mazandaran, P. O. Box 47416-95447, Babolsar, Iran*

(Dated: April 5, 2018)

Focusing on the local type primordial non-Gaussianities, we study the bispectrum and trispectrum during a non-minimal slow-roll inflation. We use the so-called  $\delta N$  formalism to investigate the super-horizon evolution of the primordial perturbations in this setup. Firstly we obtain the main equations of the model and introduce the framework of the  $\delta N$  formalism for this case. Then we give analytical expressions for the nonlinear parameters describing the non-Gaussianity in the slow-roll approximation. We analyze the bispectrum by its non-linear parameter,  $f_{NL}$ . Furthermore, we calculate  $\tau_{NL}$  and  $g_{NL}$  which are non-linear parameters characterizing the amplitude of trispectrum. Finally, by adopting a quadratic form for both the potential and non-minimal coupling (NMC) function, we test our setup in the light of Planck2015 data and constrain the model parameters space. Although the non-Gaussianity parameters are so small in this setup, this model is consistent with recent observation. We extend our analysis to see the situation in the Einstein frame and compare the results in these two frames.

**PACS numbers:** 98.80.Cq , 98.80.Es

**Key Words:** Inflation, Non-Gaussianity, Bispectrum, Trispectrum,  $\delta N$  formalism, Observational data.

## I. INTRODUCTION

Cosmological inflation has become an important arena of cosmology which can successfully address some shortcomings of the standard model such as the horizon, flatness and relics problems [4, 38, 55, 56, 59, 77]. Moreover, inflationary cosmology provides a graceful mechanism which clarifies the observed anisotropy of the CMB radiation and also explains the origin of the almost scale invariant density perturbation leading to the large scale structure formation in the universe [13, 30, 53, 54, 95]. To date, almost scale invariant spectrum is confirmed and we even know that the violation of the exact scale invariance is about 4% level [48], which is also consistent with the simplest slow-roll inflationary model. Nevertheless, the non-linear dynamics of cosmological perturbations causes non-Gaussianity of the temperature fluctuations which is one of the most important achievements of observational data [8, 49] and these observations may bring us worth information about the dynamics of inflation. Since the primordial non-Gaussianity contains a large amount of information on the cosmological dynamics (which derives the initial inflationary expansion of the universe), studying this feature of the perturbation modes is indeed an important subject and any inflationary scenario which can show the non-Gaussianity of the primordial perturbation is somehow more favorable. For these reasons, many authors studied the non-Gaussian feature of the primordial perturbations so far. For a relatively extended list of recent literature on non-Gaussianity, see [3, 5, 7, 8, 14, 15, 16, 17, 18, 19, 20, 21, 22, 26, 27, 31, 32, 36, 42, 49, 50, 57, 58, 60, 62, 63, 64, 66, 67, 68, 69,

70, 71, 72, 73, 78, 79, 80, 83, 84, 97].

The non-Gaussianities which are generated in the primordial universe can be specified by their shapes. For instance, equilateral [23] (which has a peak when all three wave numbers are in similar sizes,  $k_1 = k_2 = k_3$ ) or orthogonal [28] shapes indicate modifications of the kinetic Lagrangian of the inflaton field. However, the local shape non-Gaussianity [8, 49] (which has a peak in the squeezed limit where two wave numbers are much larger than the third one,  $k_1 = k_2 \gg k_3$ ) illustrates large super-Hubble interactions. Moreover, folded shapes [23] are arisen from modified initial conditions and intermediate shapes [24, 25] signal the existence of interacting sectors with energy scale of the Hubble order, respectively.

In order to specify an exact Gaussian distribution of perturbations from a statistical approach, all we need is the two-point correlation function (or its Fourier transform, the power spectrum) [9]. Hence the three-point correlation function, or the Bispectrum which is its Fourier transform, gives the lowest order statistics to be able to identify non-Gaussian perturbations from Gaussian ones [35, 39]. Furthermore, the higher order statistics of non-Gaussianity can be characterized by the four-point correlation function or its Fourier transform, the trispectrum [74]. Most of the research papers released so far have been focusing on constraining the non-Gaussianity of primordial fluctuations by treating the three-point correlation functions of the perturbations [49, 90, 94]. However, one can also constrain the four-point correlation functions, by increasingly exact measurements (see [10, 47, 74]). As a comprehensive study of bispectrum and trispectrum one can be referred to [11, 12]. We focus on four-point correlation function and trispectrum in this paper.

In this paper we consider an inflationary model with an ordinary scalar field non-minimally coupled to gravity and we study both bispectrum and trispectrum in

\* k.asadi@stu.umz.ac.ir

† knozari@umz.ac.ir

the local type non-Gaussianities on super-horizon scales. Moreover, we perform a transformation to Einstein frame to check the consistency conditions. We show that the results are the same as in Jordan frame, that is, we recover the small values of the non-Gaussianity parameters in this frame too. We note that as White et al. have shown, the non-Gaussianity of the curvature perturbation is identical in Jordan and Einstein frames for adiabatic perturbations in single-field inflation with a non-minimally coupled scalar field [96].

In order to obtain the non-linear parameters corresponding to bispectrum ( $f_{NL}$ ) and trispectrum ( $\tau_{NL}$  and  $g_{NL}$ ) of the model under consideration, we employ the  $\delta N$  formalism which is based on the *separate universe* assumption [60, 61, 81, 82, 88, 93]. This formalism provides a powerful tool to analyze the evolution of the curvature perturbation on scales larger than the horizon scale. As we know, on super-horizon scales we can only use the evolution of unperturbed separate universes and neglect spatial gradients. The main result of this approach is that it allows the primordial curvature perturbation to be related to the difference in the number of e-folds between the perturbed universe ( $N$ ) and the homogeneous background one ( $N_0$ ), which are calculated between an initially flat hypersurface (with  $t_*$  corresponding to the time of horizon crossing) and a final uniform energy density hypersurface (with  $t_e$  referring to the end of inflation), respectively. In other words, by applying this formalism one can only use the field fluctuations at horizon exit and the homogeneous field evolution thereafter in order to evolve curvature perturbation  $\zeta$  on super-horizon scales.

As we have mentioned, in testing the non-Gaussianity of fluctuations in an inflationary scenario, important non-linear parameters are presented such as  $f_{NL}$ ,  $\tau_{NL}$  and  $g_{NL}$  which can express the main properties of the cosmological perturbations. Therefore, confrontation of the inflationary setup with observation and constraining the model's parameters are important tasks towards recognition of more natural scenarios. The newest constraints on local non-Gaussianity to date are provided by the analysis of data from the Planck2015 satellite [2]. Planck2015 results in that the three non-linear parameters  $f_{NL}^{equil}$ ,  $f_{NL}^{ortho}$  and  $f_{NL}^{local}$ , which parameterize the overall amplitude of an equilateral, orthonormal and local shapes of the bispectrum, are constrained as

$$\begin{aligned} f_{NL}^{equil} &= -4 \pm 43, & f_{NL}^{ortho} &= -26 \pm 21, \\ f_{NL}^{local} &= 0.8 \pm 5.0, \end{aligned} \quad (1)$$

at the %68 confidence level. This represents a substantial step forward relative to the Planck2013 [1] with error bars shrinking by 43% equilateral, 46% orthogonal and 14% local shape. Also, the Planck team have performed an analysis of trispectrum shapes in the local case and beyond, and obtained that the amplitude of primordial trispectrum in the local model is constrained to be

$$g_{NL}^{local} = (-9.0 \pm 7.7) \times 10^4, \quad (2)$$

at the 68% CL. These results significantly improved the earlier best constraints on the trispectrum from WMAP [34, 40, 75, 85, 86, 87, 92] and large-scale structure [29, 37, 52]. Furthermore, the authors of [33] have reported constraint on  $g_{NL}^{local}$  from Planck2013 data as  $g_{NL}^{local} = (-13 \pm 18) \times 10^4$ . Although the more recent central amplitude agrees well with this result, however the statistical error is smaller by a factor of 2.3. This improvement is partly due to the lower noise level in Planck2015 data and partly due to usage of a more optimal estimator.

This paper is organized as follows: After introducing the model and reviewing the basic equations in Sec. II, we study the local type bispectrum and trispectrum of the curvature perturbations in Sec. III. To this end, we use the  $\delta N$  formalism and work on super-horizon scales. Then in Sec. IV, by adopting a quadratic form for the potential and non-minimal coupling function, we obtain the non-linear parameters associated to both first and second order non-Gaussianities of the model focusing on the local shapes ( $f_{NL}^{local}$ ,  $\tau_{NL}^{local}$  and  $g_{NL}^{local}$ ). After analyzing the evolution of the mentioned non-linear parameters in Sec. V, we test the model in the light of Planck data (Planck2013 for  $g_{NL}^{local}$  versus  $\tau_{NL}^{local}$  and Planck2015 for  $g_{NL}^{local}$  versus  $f_{NL}^{local}$ ) and we obtain constraints on the parameters space of the model. Furthermore, we study the non-minimal inflation in Einstein frame in section VI. Then in sections VII and VIII we present a detailed calculation of the non-linear parameters associated to bispectrum and trispectrum in Einstein frame and we study the model numerically in this frame. Finally, we give our summary and conclusions in Sec. IX.

## II. THE MODEL

We consider a model of cosmological inflation driven by a scalar field which is non-minimally coupled to the Ricci scalar and is described by the following action

$$\mathcal{S} = \int d^4x \sqrt{-g} \left[ \frac{1}{2\kappa^2} R + f(\phi)R - \frac{1}{2} \partial_\mu \phi \partial^\mu \phi - V(\phi) \right], \quad (3)$$

where  $R$  is the 4-dimensional Ricci scalar,  $\phi$  is an ordinary scalar field as inflaton and  $V(\phi)$  is its potential.  $f(\phi)$  shows an explicit non-minimal coupling of the scalar field with the Ricci scalar. Considering a spatially flat Friedmann-Robertson-Walker space-time and varying the action (3) with respect to the scalar field, results the following equation of motion

$$\ddot{\phi} + 3H\dot{\phi} + V_{,\phi} = f_{,\phi}R. \quad (4)$$

Furthermore, variation of the action (3) with respect to the metric leads to the Friedmann equation as

$$H^2 = \frac{\kappa^2}{3(1+2\kappa^2 f)} \left[ \frac{1}{2} \dot{\phi}^2 - 6H\dot{\phi}f_{,\phi} + V(\phi) \right]. \quad (5)$$

Now, we apply the slow-roll approximation to these main equations in which we assume  $\dot{\phi} \ll |3H\dot{\phi}|$  and  $\dot{\phi}^2 \ll V(\phi)$ . The equation of motion of the non-minimally coupled scalar field and the Friedmann equation in the slow-roll limit, are given respectively as

$$3H\dot{\phi} = f_{,\phi}R - V_{,\phi}, \quad (6)$$

and

$$H^2 = \frac{\kappa^2}{3(1+2\kappa^2 f)} [V - 2f_{,\phi}^2 R + 2f_{,\phi} V_{,\phi}]. \quad (7)$$

Moreover, the number of e-folds during inflationary era is defined as

$$N = \int_{t_*}^{t_e} H dt, \quad (8)$$

and takes the following expression in our setup

$$N(\phi) = \int_{\phi_*}^{\phi_e} \frac{\kappa^2 (V - 2f_{,\phi}^2 R + 2f_{,\phi} V_{,\phi})}{(1 + 2\kappa^2 f)(f_{,\phi} R - V_{,\phi})} d\phi, \quad (9)$$

where  $\phi_*$  refers to the value of the scalar field when the universe scale observed today crosses the Hubble horizon during inflation and  $\phi_e$  denotes the value of  $\phi$  when the universe scale exits the inflationary phase.

### III. LOCAL NON-GAUSSIANITY USING $\delta N$ FORMALISM

The amplitude of quantum fluctuation of the scalar field  $\phi$  (inflaton) during slow-roll inflation is given by

$$\delta\phi = \frac{H}{2\pi}. \quad (10)$$

We note that, on scales as large as the Horizon radius, since the amplitude of the field perturbation depends on the chosen gauge, its meaning is not so clear. However, choosing the flat slicing gauge, the field's perturbation equation becomes very simple and is look alike to the case without gravitational perturbation. This is because choosing this gauge the trace of the spatial curvature remains unperturbed [65]. Thus the amplitude of field perturbation can be realized as that in the flat slicing gauge and can be interpreted as the dimensionless curvature perturbation on a uniform energy density hypersurface. The primordial curvature perturbation on uniform density spatial hypersurfaces is denoted by  $\zeta$  [89]. Transformation law is determined by the following expression

$$\zeta = H\delta t, \quad (11)$$

with  $\delta t$  being the shift in time coordinate for this transformation. Applying the time derivative of the background field,  $\dot{\phi}$ , we have  $\delta t = \frac{\delta\phi}{\dot{\phi}}$  and using (10), equation (11) can be rewritten as

$$\zeta = \frac{H^2}{2\pi\dot{\phi}}. \quad (12)$$

Since the evolution path of the universe is unique, the curvature perturbation does not evolve on super-horizon scales and hence it is useful to write the perturbation amplitude in terms of the dimensionless curvature perturbation,  $\zeta$ . Stability of  $\zeta$  makes the analysis of the density perturbation during inflation with a single field model easier.

It is important to note that the statistical properties of  $\zeta$  are constrained by observations. Moreover, these properties are commonly measured in terms of  $\zeta$ 's power spectrum, bispectrum, and trispectrum. As mentioned previously, various types of non-Gaussianities are proposed, but in this paper we focus on the so-called *local-type non-Gaussianity* which is specified by the existence of a one-to-one local map between the physical curvature perturbation,  $\zeta(x)$ , and the variable which follows the Gaussian statistics,  $\zeta_G(x)$ , at respective spatial points. In other words, the curvature perturbation can be expanded as

$$\zeta(x) = \zeta_G(x) + \frac{3}{5}f_{NL}\zeta_G^2(x) + \frac{9}{25}g_{NL}\zeta_G^3(x) + \dots, \quad (13)$$

and the two-point correlation function can be determined by the power spectrum  $P_\zeta$  as

$$\langle \zeta_{\mathbf{k}_1} \zeta_{\mathbf{k}_2} \rangle \equiv (2\pi)^3 \delta^3(\mathbf{k}_1 + \mathbf{k}_2) P_\zeta(k_1). \quad (14)$$

The three point correlation function can be defined by the following expression

$$\langle \zeta_{\mathbf{k}_1} \zeta_{\mathbf{k}_2} \zeta_{\mathbf{k}_3} \rangle \equiv (2\pi)^3 \delta^3(\mathbf{k}_1 + \mathbf{k}_2 + \mathbf{k}_3) \mathcal{B}_\zeta(k_1, k_2, k_3), \quad (15)$$

where  $\mathcal{B}_\zeta$  is the bispectrum given by

$$\mathcal{B}_\zeta(k_1, k_2, k_3) = \frac{6}{5}f_{NL}[P_\zeta(k_1)P_\zeta(k_2) + P_\zeta(k_2)P_\zeta(k_3) + P_\zeta(k_3)P_\zeta(k_1)], \quad (16)$$

with  $f_{NL}$  being the non-linear parameter [49]. We emphasize that, although other types of non-Gaussianities can be generated, but focusing on super-horizon scales only leads to the local-type non-Gaussianity which is the aim of this study. To proceed further, we use the  $\delta N$  formalism which is based on the separate universe assumption [76, 81, 82, 93]. This formalism provides a powerful tool to evaluate the evolution of the curvature perturbation on super-horizon scales. Since on scales larger than the horizon spatial gradients can be neglected, each spatial point can be considered to evolve as a separate Friedmann-Robertson-Walker universe. To put it simply, super-horizon dynamics is locally characterized by the FRW universe. We choose an initially flat hypersurface at  $t = t_*$  (when the observational scales crossed the cosmological horizon) and a later uniform energy density hypersurface at  $t = t_e$  (which corresponds to the time of the end of inflation). In fact we evolve the space-time until reaching the final surface at  $t = t_e$  from the initial surface at  $t = t_*$ . After this consideration, the number of e-folds can be written as a function of the initial and

final time,  $t_*$  and  $t_e$ , on the relevant hypersurfaces in the following form

$$N(t_e, t_*, x) = \int_{t_*}^{t_e} dt H(t, x), \quad (17)$$

and the primordial curvature perturbation on the final hypersurface can be expressed as

$$\zeta(t_e, x) \equiv \delta N(t_e, x) = N(t_e, t_*, x) - N_0(t_e, t_*), \quad (18)$$

which is the heart of the  $\delta N$  formalism and

$$N_0(t_e, t_*) = \int_{t_*}^{t_e} dt H_0(t, x). \quad (19)$$

Since in an expanding universe each horizon patch is causally disconnected from the others, its evolution is defined as a local process.

By considering  $t_*$  to be the time of horizon exit ( $kc_s = aH$ ), one can write the curvature perturbation on super-horizon scales in terms of partial derivatives of  $N$  with respect to the initial field values on the flat slicing (unperturbed scalar field values at horizon exit). In fact, during the slow-roll inflation, evolution of the universe is assumed to be specified by one scalar field or more. Choosing the flat slicing gauge and considering perturbations, one can expand each scalar field to a homogeneous background and local perturbation,  $\phi_i(t_*, x) = \phi_i(t_*) + \delta\phi_i(t_*, x)$ . Therefore  $\zeta$  can be expanded in powers of  $\delta\phi$

$$\begin{aligned} \zeta(t_e, x) = & \sum_i N_{,i} \delta\phi^i + \\ & \sum_{ij} \frac{1}{2} N_{,ij} \delta\phi^i \delta\phi^j + \sum_{ijk} \frac{1}{6} N_{,ijk} \delta\phi^i \delta\phi^j \delta\phi^k + \dots \end{aligned} \quad (20)$$

where  $N$  is the number of e-folds from  $t_*$  to  $t_e$  and  $N_{,i} = \frac{\partial N}{\partial \phi_i}$  and  $\delta\phi_i$ 's are the field fluctuations on the initial flat hypersurface shortly after horizon exit,  $t_*$ . We note that this is while the initial and final hypersurfaces are remained constant. Furthermore, we emphasize that the inflaton field velocities are functions of the field position,  $\dot{\phi}(t_*, x)$ . Subsequently, even when the evolution runs away from slow-roll, the number of e-folds between the initial hypersurface and the final one is a function of the initial field values on initial flat hypersurface,  $N(t_e, \phi(t_*, x))$ .

Now employing the  $\delta N$  expansion and using the two-point function (14), one finds the dimensionless power spectrum as [81]

$$\mathcal{P}_\zeta(k_1) = N_{,i}^2 \mathcal{P}_*, \quad (21)$$

where  $\mathcal{P}_\zeta = \frac{k^3}{2\pi^2} P_\zeta$  and  $\mathcal{P}_* = \left(\frac{H_*}{2\pi}\right)^2$ . Now we proceed to the lowest order non-Gaussianity which is the three-point correlation function, or its Fourier transform, the bispectrum,  $\mathcal{B}_\zeta$ . Using the  $\delta N$  formalism, equation (15)

can be written in terms of the derivatives of  $N$  as [60]

$$\begin{aligned} \langle \zeta_{\mathbf{k}_1} \zeta_{\mathbf{k}_2} \zeta_{\mathbf{k}_3} \rangle = & \sum_{ijk} N_{,i} N_{,j} N_{,k} \langle \delta\phi_{\mathbf{k}_1}^i \delta\phi_{\mathbf{k}_2}^j \delta\phi_{\mathbf{k}_3}^k \rangle + \\ & \left( \frac{1}{2} \sum_{ijkl} N_{,i} N_{,j} N_{,kl} \langle \delta\phi_{\mathbf{k}_1}^i \delta\phi_{\mathbf{k}_2}^j (\delta\phi^k \star \delta\phi^l)_{\mathbf{k}_3} \rangle + 2 \text{ perms.} \right), \end{aligned} \quad (22)$$

where  $\star$  denotes a convolution and ?perms? denotes cyclic permutations over the momenta. This expansion of the three-point function, (22), demonstrates two distinct contributions. Its first term contributes to non-Gaussianity in the primordial curvature perturbation through the inherent non-Gaussianity of  $\delta\phi^i$ , which is generated by quantum field interactions on sub-horizon scales. Although for Gaussian perturbations, this term vanishes identically, however,  $\zeta$  can still be non-Gaussian through the second term. This second term is due to the non-linear behavior in curvature perturbation on super-horizon scales and is mostly referred to as *local-type non-Gaussianity* (one can refer to [6] for a discussion of the shape dependence of the bispectrum). Therefore, we mainly focus on this contribution which is toward our aim in this paper.

Now let us neglect the connected part of the four-point function and apply Wick's theorem which helps us to rewrite the four-point correlation functions in terms of two-point functions. Then the second contribution in (22) can be written as [15, 60]

$$\begin{aligned} & \frac{1}{2} \sum_{ijkl} N_{,i} N_{,j} N_{,kl} \langle \delta\phi_{\mathbf{k}_1}^i \delta\phi_{\mathbf{k}_2}^j (\delta\phi^k \star \delta\phi^l)_{\mathbf{k}_3} \rangle + 2 \text{ perms.} \\ & = (2\pi)^3 4\pi^4 \mathcal{P}_*^2 \frac{\sum_i k_i^3}{\prod_i k_i^3} \sum_{ij} N_{,i} N_{,j} N_{,ij} \delta^3(\mathbf{k}_1 + \mathbf{k}_2 + \mathbf{k}_3). \end{aligned} \quad (23)$$

Adopting the notation of [91], the bispectrum can be written as follows

$$\mathcal{B}_\zeta(k_1, k_2, k_3) = 4\pi^4 \mathcal{P}_\zeta^2 \frac{\sum_i k_i^3}{\prod_i k_i^3} \left( \frac{6}{5} f_{NL}(k_1, k_2, k_3) \right), \quad (24)$$

where

$$f_{NL}(k_1, k_2, k_3) = f_{NL}^{(3)}(k_1, k_2, k_3) + f_{NL}^{(4)}. \quad (25)$$

Here  $f_{NL}^{(3)}$  is the momentum dependent parameter which accounts for the sub-horizon contribution. However, since we are primarily interested in local non-Gaussianity which is confirmed on super-horizon scales, we skip over this term. Whilst  $f_{NL}^{(4)}$  is momentum independent parameter and accounts for the super-horizon contribution (one can refer to [45, 46] for more discussions).

One of our aim in this paper is to calculate  $f_{NL}^{(4)}$  for the case with a non-minimally coupled scalar field. This quantity is generally described by the following expression

$$\frac{6}{5} f_{NL}^{(4)} = \frac{\sum_{ij} N_{,i} N_{,j} N_{,ij}}{\left(\sum_k N_{,k}^2\right)^2}. \quad (26)$$

Now we describe the leading order contributions to the primordial trispectrum in a perturbative expansion for the local shape of non-Gaussianity using the  $\delta N$  formalism. To this end, we derive the four-point correlation function of the field fluctuations which is given by

$$\langle \zeta_{\mathbf{k}_1} \zeta_{\mathbf{k}_2} \zeta_{\mathbf{k}_3} \zeta_{\mathbf{k}_4} \rangle \equiv (2\pi)^3 \delta^3(\mathbf{k}_1 + \mathbf{k}_2 + \mathbf{k}_3 + \mathbf{k}_4) \mathcal{T}_\zeta(k_1, k_2, k_3, k_4), \quad (27)$$

where

$$\begin{aligned} \mathcal{T}_\zeta(k_1, k_2, k_3, k_4) = & \tau_{NL} [P_\zeta(k_{13}) P_\zeta(k_3) P_\zeta(k_4) + (11 \text{ perms.})] + \\ & \frac{54}{25} g_{NL} [P_\zeta(k_2) P_\zeta(k_3) P_\zeta(k_4) + (3 \text{ perms.})]. \end{aligned} \quad (28)$$

Now, as performed previously for the bispectrum, using the expression for the curvature perturbation (20) one can obtain these new observational parameters,  $\tau_{NL}$  and  $g_{NL}$ , in terms of the derivatives of  $N$ . The trispectrum of the primordial curvature perturbation (28) at the leading order can be written as

$$\begin{aligned} \mathcal{T}_\zeta(k_1, k_2, k_3, k_4) = & \sum_{ijk} N_{,ij} N_{,ik} N_{,j} N_{,k} [P(k_{13}) P(k_3) P(k_4) + 11 \text{ perms.}] + \\ & \sum_{ijk} N_{,ijk} N_{,i} N_{,j} N_{,k} [P(k_2) P(k_3) P(k_4) + 3 \text{ perms.}]. \end{aligned} \quad (29)$$

By comparing (28) and (29) and recalling (21) we have

$$\tau_{NL}^{local} = \frac{\sum_{ijk} N_{,ij} N_{,ik} N_{,j} N_{,k}}{\sum_l (N_{,l} N_{,l})^3}, \quad (30)$$

$$g_{NL}^{local} = \frac{25 \sum_{ijk} N_{,ijk} N_{,i} N_{,j} N_{,k}}{54 \sum_l (N_{,l} N_{,l})^3}. \quad (31)$$

We note that in order to check the local type non-Gaussianity in the trispectrum, terms with different momentum dependence are factored out and only two momentum independent non-linearity parameters,  $\tau_{NL}^{local}$  and  $g_{NL}^{local}$ , are defined. This can give the facility that observational data may be able to identify between the two parameters [74]. Up to this point we introduced the  $\delta N$  formalism in order to calculate the non-linear parameters  $f_{NL}^{local}$ ,  $\tau_{NL}^{local}$  and  $g_{NL}^{local}$ . In the next section we present the results for the case with a non-minimally coupled scalar field.

#### IV. PRIMORDIAL NON-GAUSSIANITY IN A NON-MINIMAL INFLATION

Up to this point, by considering an inflationary scenario with an inflaton field non-minimally coupled to gravity, we obtained the basic equations. Then we have presented the general form of the non-linear parameters in the local type non-Gaussianities. Now we are in the

position to calculate the local type non-Gaussianities of the primordial fluctuations in our non-minimal setup.

Using (20) the primordial curvature perturbation takes the following form in our model

$$\zeta(t_e, x) = N_{,\phi} \delta\phi + \frac{1}{2} N_{,\phi\phi} (\delta\phi)^2 + \frac{1}{6} N_{,\phi\phi\phi} (\delta\phi)^3. \quad (32)$$

As mentioned previously, in order to study local type non-Gaussianity it is enough to focus on super-horizon scales and in this region  $f_{NL}^{local}$  is defined by (26) which takes the following form in our model

$$\frac{6}{5} f_{NL}^{local} = \frac{N_{,\phi\phi}}{(N_{,\phi})^2}. \quad (33)$$

It is clear that since there is only one field and one  $\delta\phi_i$ , we have rewritten  $N_{,i}$  as  $N_{,\phi}$  and  $N_{,ii}$  as  $N_{,\phi\phi}$  for simplicity. According to the equation (9), we obtain the following relation for the first derivative of the number of e-folds with respect to the inflaton field

$$N_{,\phi} = -\kappa^2 \frac{(V - 2f_{,\phi}^2 R + 2f_{,\phi} V_{,\phi})}{(1 + 2\kappa^2 f)(V_{,\phi} - f_{,\phi} R)}. \quad (34)$$

Next, the second derivative of  $N$  gives

$$\begin{aligned} N_{,\phi\phi} = & \kappa^2 \left( \frac{2\kappa^2 f_{,\phi} (V - 2f_{,\phi}^2 R + 2f_{,\phi} V_{,\phi})}{(1 + 2\kappa^2 f)^2 (V_{,\phi} - f_{,\phi} R)} \right) - \\ & \kappa^2 \left( \frac{V_{,\phi} - 4f_{,\phi} f_{,\phi\phi} R + 2f_{,\phi\phi} V_{,\phi} + 2f_{,\phi} V_{,\phi\phi}}{(1 + 2\kappa^2 f)(V_{,\phi} - f_{,\phi} R)} \right) + \\ & \kappa^2 \left( \frac{(V - 2f_{,\phi}^2 R + 2f_{,\phi} V_{,\phi})(V_{,\phi\phi} - f_{,\phi\phi} R)}{(1 + 2\kappa^2 f)(V_{,\phi} - f_{,\phi} R)^2} \right). \end{aligned} \quad (35)$$

Applying (34) and (35) in the main equation for  $f_{NL}^{local}$ , that is, (33), we obtain our first non-linear parameter in the local configuration as

$$\begin{aligned} \frac{6}{5} f_{NL}^{local} = & \frac{(1 + 2\kappa^2 f)(V_{,\phi} - f_{,\phi} R)}{\kappa^2 (V - 2f_{,\phi}^2 R + 2f_{,\phi} V_{,\phi})} \times \\ & \left[ \frac{4f_{,\phi} f_{,\phi\phi} R - V_{,\phi} - 2f_{,\phi\phi} V_{,\phi} - 2f_{,\phi} V_{,\phi\phi}}{V - 2f_{,\phi}^2 R + 2f_{,\phi} V_{,\phi}} + \right. \\ & \left. \frac{2\kappa^2 f_{,\phi}}{1 + 2\kappa^2 f} + \frac{V_{,\phi\phi} - f_{,\phi\phi} R}{V_{,\phi} - f_{,\phi} R} \right]. \end{aligned} \quad (36)$$

Then we calculate the trispectrum of the model. According to equations (30) we have

$$\tau_{NL}^{local} = \frac{(N_{,\phi\phi})^2}{(N_{,\phi})^4}, \quad (37)$$

which leads to the following relation in our model

$$\begin{aligned} \tau_{NL}^{local} = & \frac{(1 + 2\kappa^2 f)^2 (V_{,\phi} - f_{,\phi} R)^2}{\kappa^4 (V - 2f_{,\phi}^2 R + 2f_{,\phi} V_{,\phi})^4} \left[ 4f_{,\phi} f_{,\phi\phi} R - \right. \\ & V_{,\phi} - 2f_{,\phi\phi} V_{,\phi} - 2f_{,\phi} V_{,\phi\phi} + (V - 2f_{,\phi}^2 R + 2f_{,\phi} V_{,\phi}) \\ & \left. \times \left( \frac{2\kappa^2 f_{,\phi}}{1 + 2\kappa^2 f} + \frac{V_{,\phi\phi} - f_{,\phi\phi} R}{V_{,\phi} - f_{,\phi} R} \right) \right]^2. \end{aligned} \quad (38)$$

Also equation (31) results the following form for  $g_{NL}^{local}$

$$\frac{54}{25}g_{NL}^{local} = \frac{N_{,\phi\phi\phi}}{(N_{,\phi})^3}. \quad (39)$$

Thus, in order to obtain  $g_{NL}^{local}$ , we should first obtain the third derivative of  $N$  which takes the following expression

$$\begin{aligned} N_{,\phi\phi\phi} = & \left[ V_{,\phi\phi} - 4f_{,\phi\phi}^2 R - 4f_{,\phi} f_{,\phi\phi\phi} R + 2f_{,\phi\phi\phi} V_{,\phi} + 4f_{,\phi\phi} V_{,\phi\phi} + 2f_{,\phi} V_{,\phi\phi\phi} - \left( \frac{2\kappa^2 f_{,\phi}}{1+2\kappa^2 f} + \frac{V_{,\phi\phi} - f_{,\phi\phi} R}{V_{,\phi} - f_{,\phi} R} \right) \times \right. \\ & (V_{,\phi} - 4f_{,\phi} f_{,\phi\phi} R + 2f_{,\phi\phi} V_{,\phi} + 2f_{,\phi} V_{,\phi\phi}) - \left( \frac{2\kappa^2 f_{,\phi\phi}}{1+2\kappa^2 f} - \frac{4\kappa^4 f_{,\phi}^2}{(1+2\kappa^2 f)^2} + \frac{V_{,\phi\phi\phi} - f_{,\phi\phi\phi} R}{V_{,\phi} - f_{,\phi} R} - \frac{(V_{,\phi\phi} - f_{,\phi\phi} R)^2}{(V_{,\phi} - f_{,\phi} R)^2} \right) \times \\ & \left. (V - 2f_{,\phi}^2 R + 2f_{,\phi} V_{,\phi}) \right] \left[ \frac{-\kappa^2}{(1+2\kappa^2 f)(V_{,\phi} - f_{,\phi} R)} \right] + \left[ \frac{\kappa^2}{(1+2\kappa^2 f)(V_{,\phi} - f_{,\phi} R)} \left( \frac{2\kappa^2 f_{,\phi}}{1+2\kappa^2 f} + \frac{V_{,\phi\phi} - f_{,\phi\phi} R}{V_{,\phi} - f_{,\phi} R} \right) \right] \times \\ & \left[ V_{,\phi} - 4f_{,\phi} f_{,\phi\phi} R + 2f_{,\phi\phi} V_{,\phi} + 2f_{,\phi} V_{,\phi\phi} - \left( \frac{2\kappa^2 f_{,\phi}}{1+2\kappa^2 f} + \frac{V_{,\phi\phi} - f_{,\phi\phi} R}{V_{,\phi} - f_{,\phi} R} \right) (V - 2f_{,\phi}^2 R + 2f_{,\phi} V_{,\phi}) \right]. \end{aligned} \quad (40)$$

Finally, using (39), the trispectrum non-linear parameter

in a non-minimal inflation reads

$$\begin{aligned} \frac{54}{25}g_{NL}^{local} = & \left[ V_{,\phi\phi} - 4f_{,\phi\phi}^2 R - 4f_{,\phi} f_{,\phi\phi\phi} R + 2f_{,\phi\phi\phi} V_{,\phi} + 4f_{,\phi\phi} V_{,\phi\phi} + 2f_{,\phi} V_{,\phi\phi\phi} - \right. \\ & (V_{,\phi} - 4f_{,\phi} f_{,\phi\phi} R + 2f_{,\phi\phi} V_{,\phi} + 2f_{,\phi} V_{,\phi\phi}) \left( \frac{2\kappa^2 f_{,\phi}}{1+2\kappa^2 f} + \frac{V_{,\phi\phi} - f_{,\phi\phi} R}{V_{,\phi} - f_{,\phi} R} \right) - (V - 2f_{,\phi}^2 R + 2f_{,\phi} V_{,\phi}) \times \\ & \left. \left( \frac{2\kappa^2 f_{,\phi\phi}}{1+2\kappa^2 f} - \frac{4\kappa^4 f_{,\phi}^2}{(1+2\kappa^2 f)^2} + \frac{V_{,\phi\phi\phi} - f_{,\phi\phi\phi} R}{V_{,\phi} - f_{,\phi} R} - \frac{(V_{,\phi\phi} - f_{,\phi\phi} R)^2}{(V_{,\phi} - f_{,\phi} R)^2} \right) \right] \left[ \frac{(1+2\kappa^2 f)^2 (V_{,\phi} - f_{,\phi} R)^2}{\kappa^4 (V - 2f_{,\phi}^2 R + 2f_{,\phi} V_{,\phi})^3} \right] + \\ & \left[ V_{,\phi} - 4f_{,\phi} f_{,\phi\phi} R + 2f_{,\phi\phi} V_{,\phi} + 2f_{,\phi} V_{,\phi\phi} - \left( \frac{2\kappa^2 f_{,\phi}}{1+2\kappa^2 f} + \frac{V_{,\phi\phi} - f_{,\phi\phi} R}{V_{,\phi} - f_{,\phi} R} \right) (V - 2f_{,\phi}^2 R + 2f_{,\phi} V_{,\phi}) \right] \times \\ & \left. \left( \frac{2\kappa^2 f_{,\phi}}{1+2\kappa^2 f} + \frac{V_{,\phi\phi} - f_{,\phi\phi} R}{V_{,\phi} - f_{,\phi} R} \right) \left[ -\frac{(1+2\kappa^2 f)^2 (V_{,\phi} - f_{,\phi} R)^2}{\kappa^4 (V - 2f_{,\phi}^2 R + 2f_{,\phi} V_{,\phi})^3} \right]. \end{aligned} \quad (41)$$

Up to here we have calculated the main equations of the setup toward analyzing both bispectrum and trispectrum of the local-type non-Gaussianity. Now we are in the position to proceed further by specifying the form of the potential,  $V(\phi)$ , and the non-minimal coupling function,  $f(\phi)$ . In this regard we consider a quadratic form for these functions of the scalar field as,  $V(\phi) = \frac{1}{2}m_\phi^2\phi^2$  and  $f(\phi) = \frac{1}{2}\xi\phi^2$ . Adopting these functions in main equations of section (II) leads to the following number of e-folds in our scenario

$$N(\phi) = - \int_{\phi}^{\phi_e} \frac{\kappa^2 (\frac{1}{2}m_\phi^2\phi^2 - 2\xi^2\phi^2 R + 2\xi\phi^2 m_\phi^2)}{(m_\phi^2\phi - \xi\phi R)(1 + \kappa^2\xi\phi^2)} d\phi, \quad (42)$$

which gives

$$N(\phi) = \left( \frac{m_\phi^2 - 4\xi^2 R + 4\xi m_\phi^2}{4\xi(\xi R - m_\phi^2)} \right) \ln \left( \frac{1 + \kappa^2\xi\phi_e^2}{1 + \kappa^2\xi\phi^2} \right), \quad (43)$$

Through Eq. (43) we can obtain the value of the field during the slow-roll inflation in terms of the number of e-folds

$$\phi(N) = \frac{\left( -1 + (1 + \kappa^2\xi\phi_e^2) e^{\frac{4N(-m_\phi^2 + \xi R)\xi}{4\xi^2 R - 4m_\phi^2\xi - m_\phi^2}} \right)^{\frac{1}{2}}}{\xi^{\frac{1}{2}}\kappa}. \quad (44)$$

Moreover, adopting the mentioned forms of  $V(\phi)$  and  $f(\phi)$ , equation (36) results the following expression for

the local non-linear parameter,  $f_{NL}^{local}$

$$\frac{6}{5}f_{NL}^{local} = \left[ \frac{m_\phi^2\phi - 4\xi^2\phi R + 4\xi m_\phi^2\phi}{\frac{1}{2}m_\phi^2\phi^2 - 2\xi^2\phi^2 R + 2\xi\phi^2 m_\phi^2} + \frac{-m_\phi^2 + \xi R}{m_\phi^2\phi - \xi\phi R} - \frac{2\kappa^2\xi\phi}{1 + \kappa^2\xi\phi^2} \right] (1 + \kappa^2\xi\phi^2)(m_\phi^2\phi - \xi\phi R) \times \left[ \kappa^2 \left( \frac{1}{2}m_\phi^2\phi^2 - 2\xi^2\phi^2 R + 2\xi\phi^2 m_\phi^2 \right) \right]^{-1}. \quad (45)$$

Furthermore, the local non-linear parameters associated

to the trispectrum of the model (38) and (41), finally are given by

$$\tau_{NL}^{local} = \left( \frac{m_\phi^2\phi - 4\xi^2\phi R + 4\xi m_\phi^2\phi}{\frac{1}{2}m_\phi^2\phi^2 - 2\xi^2\phi^2 R + 2\xi\phi^2 m_\phi^2} + \frac{-m_\phi^2 + \xi R}{m_\phi^2\phi - \xi\phi R} - \frac{2\kappa^2\xi\phi}{1 + \kappa^2\xi\phi^2} \right)^2 (m_\phi^2\phi - \xi\phi R)^2 \times (1 + \kappa^2\xi\phi^2)^2 \left[ \kappa^2 \left( \frac{1}{2}m_\phi^2\phi^2 - 2\xi^2\phi^2 R + 2\xi\phi^2 m_\phi^2 \right) \right]^{-2}, \quad (46)$$

and

$$\frac{54}{25}g_{NL}^{local} = \left[ m_\phi^2 - 4\xi^2 R + 4\xi m_\phi^2 - (m_\phi^2\phi - 4\xi^2\phi R + 4\xi m_\phi^2\phi) \left( \frac{2\kappa^2\xi\phi}{1 + \kappa^2\xi\phi^2} + \frac{m_\phi^2 - \xi R}{m_\phi^2\phi - \xi\phi R} \right) - \left( \frac{1}{2}m_\phi^2\phi^2 - 2\xi^2\phi^2 R + 2\xi\phi^2 m_\phi^2 \right) \left( \frac{2\kappa^2\xi}{1 + \kappa^2\xi\phi^2} - \frac{4\kappa^4\xi^2\phi^2}{(1 + \kappa^2\xi\phi^2)^2} - \frac{(m_\phi^2 - \xi R)^2}{(m_\phi^2\phi - \xi\phi R)^2} \right) \right] (1 + \kappa^2\xi\phi^2)^2 (m_\phi^2\phi - \xi\phi R)^2 \times \left[ \kappa^4 \left( \frac{1}{2}m_\phi^2\phi^2 - 2\xi^2\phi^2 R + 2\xi\phi^2 m_\phi^2 \right)^2 \right]^{-1} - \kappa^8 \left( \frac{1}{2}m_\phi^2\phi^2 - 2\xi^2\phi^2 R + 2\xi\phi^2 m_\phi^2 \right)^3 \left( \frac{2\kappa^2\xi\phi}{1 + \kappa^2\xi\phi^2} + \frac{m_\phi^2 - \xi R}{m_\phi^2\phi - \xi\phi R} \right) \times \left[ m_\phi^2\phi - 4\xi^2\phi R + 4\xi m_\phi^2\phi - \left( \frac{2\kappa^2\xi\phi}{1 + \kappa^2\xi\phi^2} + \frac{m_\phi^2 - \xi R}{m_\phi^2\phi - \xi\phi R} \right) \left( \frac{1}{2}m_\phi^2\phi^2 - 2\xi^2\phi^2 R + 2\xi\phi^2 m_\phi^2 \right) \right] \times \left[ (1 + \kappa^2\xi\phi^2)(m_\phi^2\phi - \xi\phi R) \right]^{-4}. \quad (47)$$

Now one can easily substitute the field value (44) in (45), (46) and (47) to obtain the intended non-linear parameters as a function of  $N$  (which imply the level of non-Gaussianity in both bispectrum and trispectrum to be depended on the non-minimal coupling strength and the number of e-folds). In what follows we perform some numerical analysis on the model's parameters space and draw the relevant figures for  $f_{NL}^{local}$ ,  $\tau_{NL}^{local}$  and  $g_{NL}^{local}$  to see the behaviors of these quantities intuitively. Furthermore, we eventually test our results in the light of Planck observational data.

## V. TESTING THE EVOLUTION OF THE NON-LINEAR PARAMETERS IN CONFRONTATION WITH OBSERVATION

In previous section we obtained the non-linear parameters corresponding to both the first and higher order of non-Gaussianity. Eq. (45) shows how the first level of non-Gaussianity,  $f_{NL}^{local}$ , depends on the inflaton field and non-minimal coupling parameter. Since the scalar field  $\phi$  is a function of the number of e-folds (through equation (44)), we can depict the evolution of  $f_{NL}^{local}$  in  $\xi$  and  $N$  space. In this regard, we should obtain the value of the

inflaton at the end of inflation,  $\phi_{end}$ .

We note that during the inflationary era, the evolution of the Hubble parameter is so slow, so that in this era the conditions  $\epsilon \ll 1$  and  $\eta \ll 1$  are satisfied. As one of these two slow-roll parameters reaches unity, the inflation phase terminates. Thus by studying the evolution of these parameters, one can find the value of the inflaton field for which the inflation ends ( $\epsilon$  or  $\eta$  reach unity). Using the definition of the slow-roll parameter,  $\epsilon = -\frac{\dot{H}}{H^2}$  we obtain the following expression

$$\epsilon = \frac{f_{,\phi}(f_{,\phi}R - V_{,\phi})}{(V - 2f_{,\phi}^2 R + 2f_{,\phi}V_{,\phi})} + \left( \frac{1 + 2\kappa^2 f}{2\kappa^2} \right) \times \frac{(V_{,\phi} - 4f_{,\phi}f_{,\phi\phi}R + 2f_{,\phi\phi}V_{,\phi} + 2f_{,\phi}V_{,\phi\phi})(V_{,\phi} - f_{,\phi}R)}{(V - 2f_{,\phi}^2 R + 2f_{,\phi}V_{,\phi})^2}, \quad (48)$$

and also  $\eta = -\frac{\ddot{H}}{H\dot{H}}$  gives

$$\eta = 2\epsilon - \frac{\dot{\epsilon}}{H\epsilon}. \quad (49)$$

Fig. 1 shows the behavior of  $\epsilon$  versus  $\phi$  and  $\xi$ . This figure confirms that the value of the field to have  $\epsilon = 1$ , that is,  $\phi_e$ , is directly dependant on the non-minimal coupling

parameter,  $\xi$ . This relationship is given by the following expression

$$\phi_e = \pm \frac{\sqrt{2(\xi R - m_\phi^2)(4\xi^2 R - m_\phi^2 - 4\xi m_\phi^2)}}{\kappa(4\xi^2 R - m_\phi^2 - 4\xi m_\phi^2)}. \quad (50)$$

In fact for smaller values of  $\xi$ , inflation ends sooner (that is, it occurs in larger values of  $\phi$  for large field inflation). We continue our analysis by adopting  $\kappa = 1$  and  $m = 0.4$ . Using these values, we obtain  $\phi_e \simeq \pm \frac{0.7\sqrt{25\xi-4}}{25\xi^2-1-4\xi}$ . To have positive  $\phi_e$  for  $0 \leq \xi \leq \frac{1}{6}$  (we restrict ourselves to this range of  $\xi$ ), we choose the minus sign for this relation. After obtaining the field value at the end of inflation, now we are in the position to study the non-Gaussianity of the model at hand through its non-linear parameters. Fig. 2 demonstrates the relation between  $f_{NL}^{local}$  and parameters  $\xi$  and  $N$  intuitively. This figure shows that for any value of  $\xi$ , the absolute value of  $f_{NL}^{local}$  increases during the inflationary era. This property is more clarified in the left panel of Fig. 3, which shows the evolution of  $f_{NL}^{local}$  in the number of e-folds space for various values of  $\xi$ . We note that in our numerical study the values of  $m_\phi$  and  $\phi_e$  are chosen so that the inflation phase terminates gracefully about the end of inflation (which is equivalent to  $N = 0$  in our setup). For instance, we have set  $m_\phi = 0.4$  which results in  $\phi_e \simeq -\frac{0.7\sqrt{25\xi-4}}{25\xi^2-1-4\xi}$ . The right panel of Fig. 3 also shows this evolution in the  $\xi$  space around the end of inflation. As an important result we can see from the left panel of Fig. 3 that the first order non-Gaussian effect is almost constant and weak at the initial stage of the inflationary era and grows gradually to values of order unity at the time of horizon crossing.

Now we proceed further by investigating evolution of the higher order non-linear parameters of local shapes,  $\tau_{NL}^{local}$  and  $g_{NL}^{local}$ . Eqs. (46) and (47) show how the second and third levels of non-Gaussianity depend on the inflation field and the non-minimal coupling parameter. Again we can depict the behavior of  $\tau_{NL}^{local}$  and  $g_{NL}^{local}$  in  $\xi$  and  $N$  space by using Eq. (44). These behaviors are depicted in Figs. 4 and 6. Comparing Figs. 2 and 4 shows that the first and second order of non-Gaussianities behave in the same way as the relation  $\tau_{NL} = (\frac{6}{5}f_{NL})^2$  shows. Also it can be seen from Fig. 6 that  $g_{NL}^{local}$  grows rapidly towards the end of inflation but stays small even in this situation. Furthermore, the behavior of the trispectrum non-linear parameters during expansion of the universe are depicted in the left panels of Figs. 5 and 7. In order to see the influence of the non-minimal coupling parameter on the level of trispectrum, the right panels of Figs. 5 and 7 have been plotted about the end of inflation.

After illustrating the evolution of bispectrum and trispectrum separately, now we are in the position to constrain the model with recent observational data. In this regard, we explore the behavior of the  $f_{NL}$  versus  $g_{NL}$  with the local configuration in the background of the Planck2015 data to see the viability of this theoretical model in confrontation with the recent observations.

This behavior is shown in Fig. 8 which confirms that although our non-Gaussianity result in non-minimal inflation is somehow small, however it is well inside the confidence region allowed by the Planck observations. We also note that this figure is depicted about the end of inflation and for  $0 < \xi \leq \frac{1}{6}$ . Confronting these evolutions and the Planck2015 data, we find the values of the non-minimal coupling parameter for which the model is consistent. As it is clear from the Fig. 8, our model is consistent with observation for all chosen values of  $\xi$ .

Moreover, as mentioned previously, with the trispectrum or the 4-point correlation function of the CMB anisotropies [41], we are able to evaluate the second and third order non-Gaussian parameters  $\tau_{NL}$  and  $g_{NL}$ . Using the correlations between (square temperature)-(square temperature) and cubic (temperature)-(temperature) anisotropies, the authors in [33] have reported measurements of the kurtosis power spectra of the CMB temperature as mapped by Planck2013. In combination with noise simulations, they have found the best joint estimates to be  $\tau_{NL}^{local} = (0.3 \pm 0.9) \times 10^4$  and  $g_{NL}^{local} = (-1.2 \pm 2.8) \times 10^5$ . They have also obtained  $g_{NL}^{local} = (-1.3 \pm 1.8) \times 10^5$  if  $\tau_{NL}^{local} = 0$ . Their analysis shows that  $\tau_{NL}^{local}$  and  $g_{NL}^{local}$  are consistent with zero for all the combinations. Using the results of [33], we can study the trispectrum parameters of non-Gaussianity and constrain the model with observation. Fig. 9 shows the amplitude of  $\tau_{NL}^{local}$  versus  $g_{NL}^{local}$  for local configuration of non-Gaussianity for a quadratic potential and the non-minimal coupling function as  $f(\phi) \sim \xi\phi^2$  in the background of Planck2013 data. This figure confirms that although the non-Gaussianity in the non-minimal inflation is almost small, however it is well inside the region allowed by the Planck observations. Confronting these behaviors and the Planck2013 data, we find that the model is consistent with observation for all values of  $\xi$ .

## VI. ANALYSIS IN EINSTEIN FRAME

Now we can move to the Einstein frame with a conformal transformation as [43, 44, 51]

$$\hat{g}_{\mu\nu} = \Omega^2 g_{\mu\nu}, \quad (51)$$

where the parameter  $\Omega$  is given by the following expression

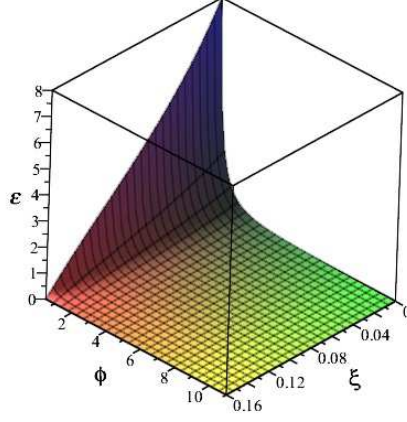
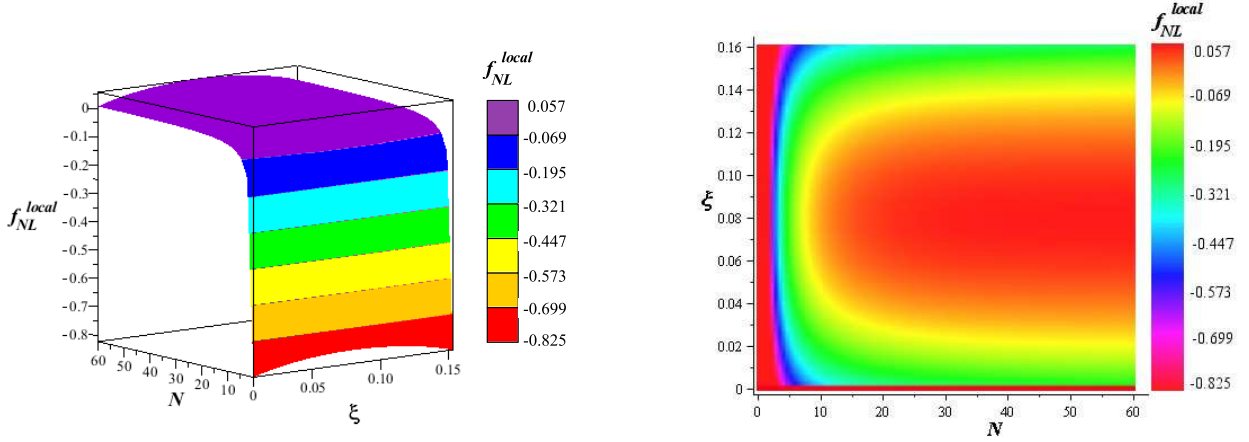
$$\Omega^2 = (1 + 2\kappa^2 f(\phi)). \quad (52)$$

In Einstein frame the new scalar field is redefined as follows

$$\frac{d\hat{\phi}}{d\phi} = \left( \frac{(1 + 2\kappa^2 f) + 6\kappa^2 f_{,\phi}^2}{(1 + 2\kappa^2 f)^2} \right)^{\frac{1}{2}}. \quad (53)$$

We further define a new scalar potential  $\hat{V}$  by

$$\hat{V}(\hat{\phi}) = \Omega^{-4} V(\phi), \quad (54)$$

FIG. 1. The behavior of  $\epsilon$  versus  $\phi$  and  $\xi$ .FIG. 2. The non-linear parameter  $f_{NL}^{local}$  as a function of the non-minimal coupling parameter  $\xi$  and the number of e-folds  $N$ .

which gives

$$\hat{V}(\hat{\phi}) = \frac{V(\phi)}{(1 + 2\kappa^2 f)^2}, \quad (55)$$

Furthermore, the action (3) in this frame becomes as

$$S_E = \int d^4x \sqrt{-\hat{g}} \left[ \frac{1}{2\kappa^2} \hat{R} - \frac{1}{2} \partial_\mu \hat{\phi} \partial^\mu \hat{\phi} - \hat{V}(\hat{\phi}) \right]. \quad (56)$$

The dynamics of the model is given by the Friedmann equation which takes the following form in Einstein frame

$$\hat{H}^2 = \frac{\kappa^2}{3} \left[ \frac{1}{2} \left( \frac{d\hat{\phi}}{d\hat{t}} \right)^2 + \hat{V}(\hat{\phi}) \right], \quad (57)$$

where we defined  $\hat{a}(\hat{t}) = (1 + 2\kappa^2 f(\phi))^{\frac{1}{2}} a(t)$  and  $\hat{t} = (1 + 2\kappa^2 f(\phi))^{\frac{1}{2}} t$ . The equation of motion of the scalar field in Einstein frame is given by

$$\ddot{\hat{\phi}} + 3\hat{H}\dot{\hat{\phi}} + \hat{V}_{,\hat{\phi}} = 0, \quad (58)$$

where a dot marks a derivative with respect to  $\hat{t}$ . With slow-roll approximations as  $\left(\frac{d\hat{\phi}}{d\hat{t}}\right)^2 \ll \hat{V}(\hat{\phi})$  and  $\left(\frac{d^2\hat{\phi}}{d\hat{t}^2}\right) \ll |3\hat{H}\frac{d\hat{\phi}}{d\hat{t}}|$ , we find

$$\hat{H}^2 = \frac{\kappa^2}{3} \hat{V}(\hat{\phi}), \quad (59)$$

and

$$3\hat{H}\frac{d\hat{\phi}}{d\hat{t}} + \frac{d\hat{V}}{d\hat{\phi}} = 0. \quad (60)$$

The number of e-folds with a non-minimally coupled scalar field in Einstein frame is given by

$$\hat{N} = -\kappa^2 \int_{\hat{\phi}_*}^{\hat{\phi}_e} \frac{\hat{V}}{\hat{V}_{,\hat{\phi}}} d\hat{\phi}, \quad (61)$$

which can be rewritten as

$$\hat{N} = -\kappa^2 \int \frac{\hat{V}}{\left(\frac{d\hat{V}}{d\hat{\phi}}\right)} \left(\frac{d\hat{\phi}}{d\hat{\phi}}\right)^2 d\hat{\phi}, \quad (62)$$

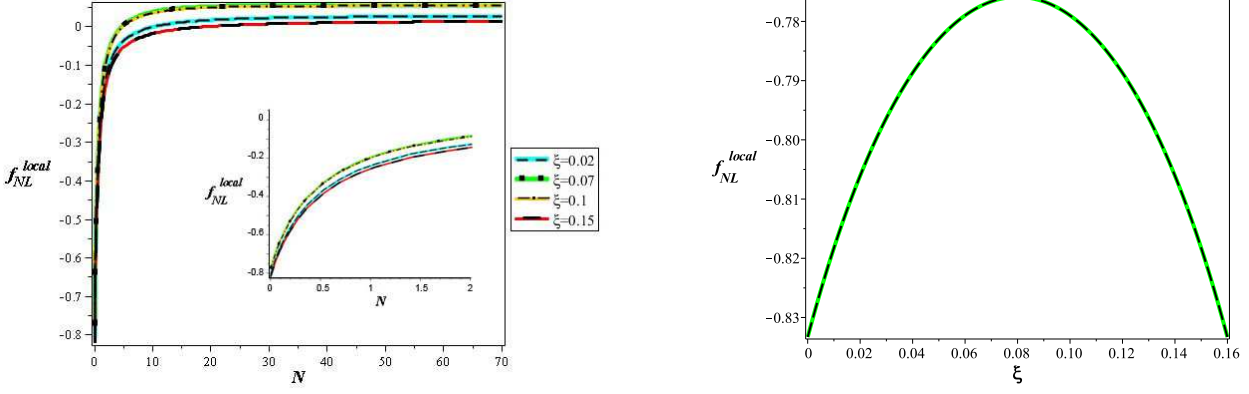


FIG. 3. Left Panel: The non-linear parameter  $f_{NL}^{local}$  for the local type non-Gaussianity versus the number of e-folds for various values of the non-minimal coupling parameter. Right Panel: The non-linear parameter  $f_{NL}^{local}$  for the local type non-Gaussianity as a function of the non-minimal coupling parameter about the time that cosmological scales exit the Hubble horizon.

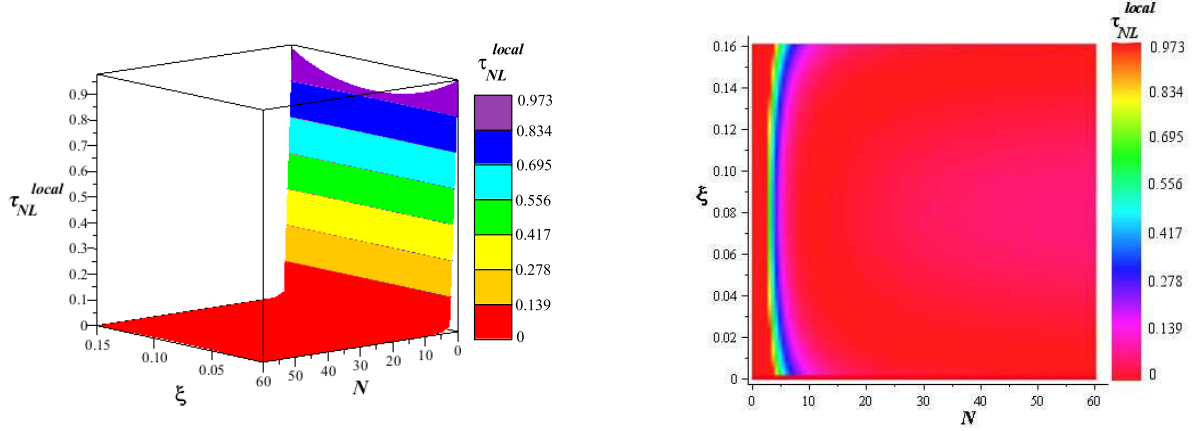


FIG. 4. The non-linear parameter  $\tau_{NL}^{local}$  as a function of the non-minimal coupling parameter  $\xi$  and the number of e-folds  $N$ .

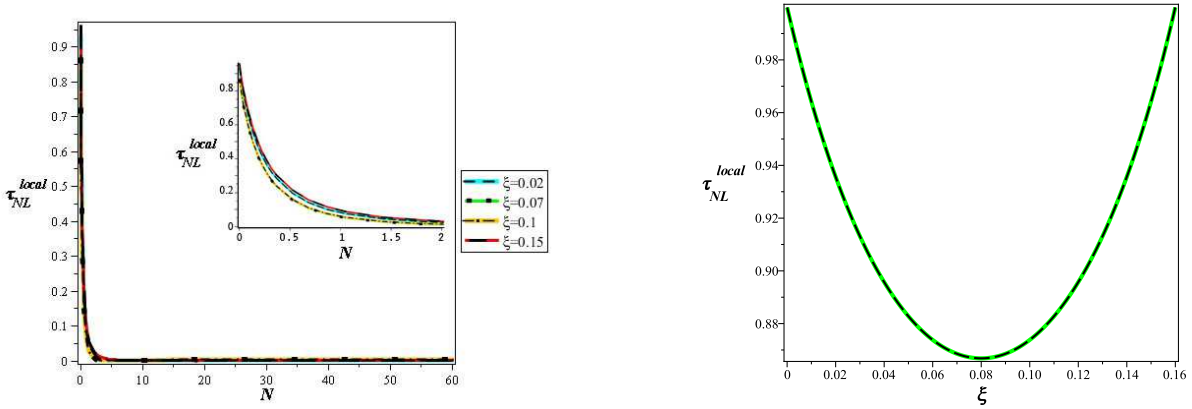


FIG. 5. Left Panel: The non-linear parameter  $\tau_{NL}^{local}$  for the local type non-Gaussianity versus the number of e-folds for various values of the non-minimal coupling parameter. Right Panel: The non-linear parameter  $\tau_{NL}^{local}$  for the local type non-Gaussianity as a function of the non-minimal coupling parameter about the time that cosmological scales exit the Hubble horizon.

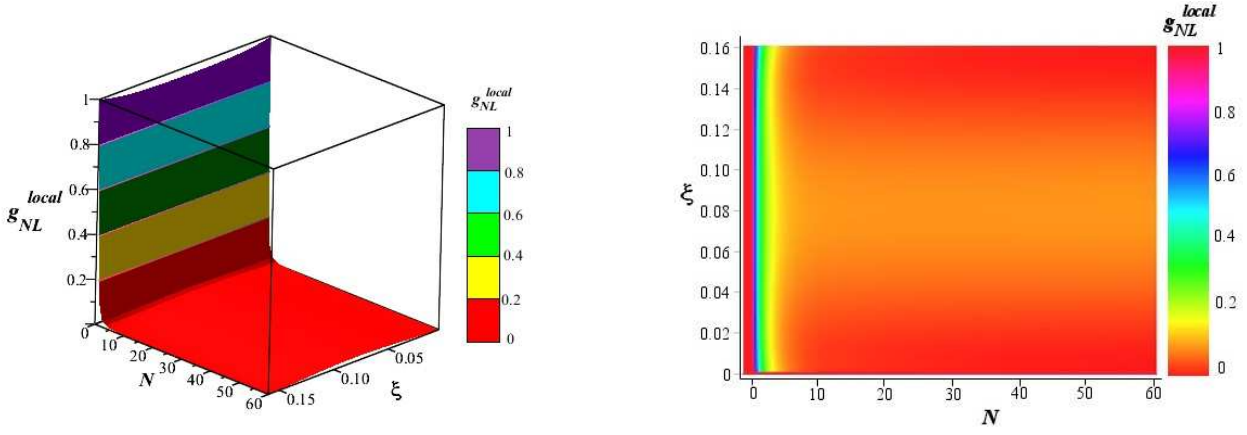


FIG. 6. The non-linear parameter  $g_{NL}^{local}$  as a function of the non-minimal coupling parameter  $\xi$  and the number of e-folds  $N$ .

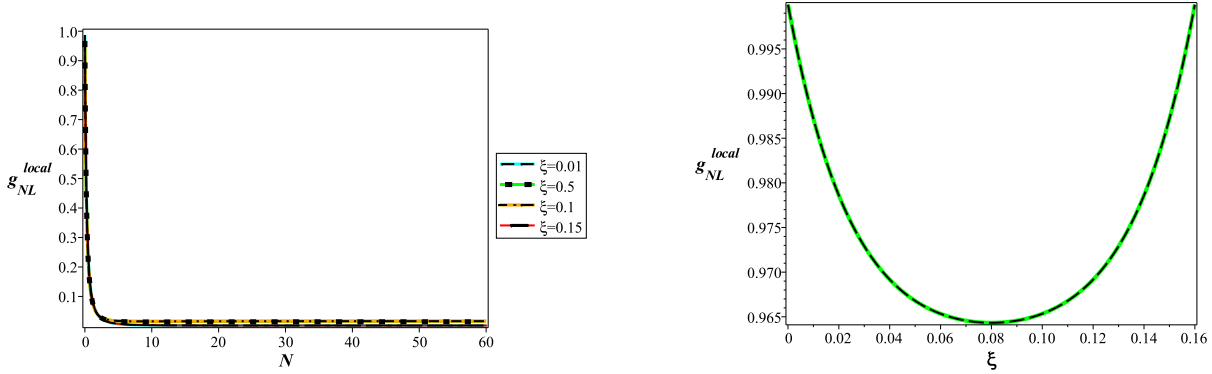


FIG. 7. Left Panel: The non-linear parameter  $g_{NL}^{local}$  for the local type non-Gaussianity versus the number of e-folds for various values of the non-minimal coupling parameter. Right panel: The non-linear parameter  $g_{NL}^{local}$  for the local type non-Gaussianity as a function of the non-minimal coupling parameter about the time that cosmological scales exit the Hubble horizon.

where we have used  $\frac{d\hat{V}}{d\phi} = \frac{d\hat{V}}{d\phi} \frac{d\phi}{d\phi}$ . Finally the number of e-folds in Einstein frame becomes

$$\hat{N} = -\kappa^2 \int_{\phi_*}^{\phi_e} \frac{V \left( (1 + 2\kappa^2 f) + 6\kappa^2 f_{,\phi}^2 \right)}{(1 + 2\kappa^2 f) [V_{,\phi} (1 + 2\kappa^2 f) - 4\kappa^2 V f_{,\phi}]} d\phi. \quad (63)$$

Now we study bispectrum and trispectrum of perturbations during a non-minimal slow-roll inflation in Einstein frame.

## VII. PRIMORDIAL NON-GAUSSIANITY IN EINSTEIN FRAME

The general form of the non-linear parameters in the local type non-Gaussianities have been presented in section 3. Now we calculate the local type non-Gaussianities of the primordial fluctuations in Einstein frame. To study local non-Gaussianities, it is enough to focus on super-horizon scales and in this region the non-linear parameters regarding to the bispectrum and trispectrum, that is,

$f_{NL}^{local}$ ,  $\tau_{NL}^{local}$  and  $g_{NL}^{local}$ , are defined by Eqs. (33), (38) and (39). Thus, in order to obtain these non-Gaussian parameters, we should obtain the first, second and third derivatives of the number of e-folds with respect to the scalar field (see Appendix A). The results for the non-linear parameters in Einstein frame are given in Appendix B. After calculating the main equations of the model to analyze both bispectrum and trispectrum of the local-type non-Gaussianities in Einstein frame, now we are in the position to proceed further by specifying the form of the potential. The potential in the Einstein frame is related to the potential in Jordan frame through Eq. (55). Similar to section 4, we continue our treatment by considering the quadratic form of the functions  $V$  and  $f$  as  $V(\phi) = \frac{1}{2}m_\phi^2\phi^2$  and  $f(\phi) = \frac{1}{2}\xi\phi^2$ . So, the potential in Einstein frame is given by

$$\hat{V}(\hat{\phi}) = \frac{m_\phi^2\phi^2}{2(1 + \kappa^2\xi\phi^2)^2}. \quad (64)$$

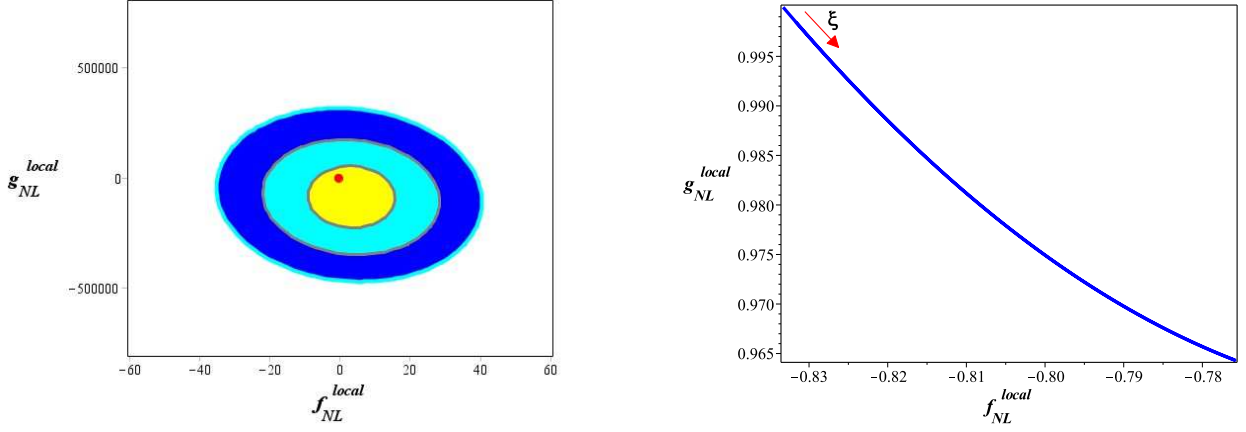


FIG. 8. The amplitude of  $g_{NL}^{local}$  versus  $f_{NL}^{local}$  for local configuration of non-Gaussianity in the background of Planck2015 data. These figures are plotted about the end of inflation for a quadratic potential and the non-minimal coupling function as  $f(\phi) \sim \xi\phi^2$ . We note that the red spot in this figure shows the position of our result in the background of the observational data. The right panel highlights more details of  $g_{NL}^{local}$  versus  $f_{NL}^{local}$  in terms of  $\xi$ .

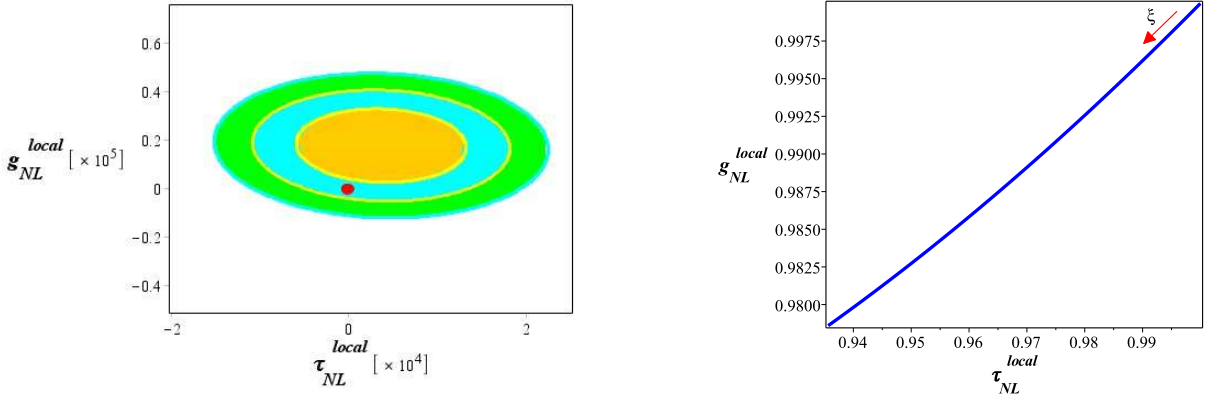


FIG. 9. The amplitude of  $g_{NL}^{local}$  versus  $\tau_{NL}^{local}$  for local configuration of non-Gaussianity in the background of Planck2013 data. These figures are plotted about the end of inflation for a quadratic potential and the non-minimal coupling function as  $f(\phi) \sim \xi\phi^2$ . We note that the red spot in this figure shows the position of our result in the background of the observational data. The right panel highlights more details of  $g_{NL}^{local}$  versus  $\tau_{NL}^{local}$  in terms of  $\xi$ .

With these choices, the number of e-folds in Einstein frame is as follows

$$\hat{N}(\phi) = \frac{3\xi + 1}{4\xi} \ln \left[ \frac{\kappa^2 \xi \phi_e^2 - 1}{\kappa^2 \xi \phi^2 - 1} \right] + \frac{3}{4} \ln \left[ \frac{\kappa^2 \xi \phi_e^2 + 1}{\kappa^2 \xi \phi^2 + 1} \right]. \quad (65)$$

The value of the field during the slow-roll inflation in Einstein frame in terms of the number of e-folds is given by

$$\phi(\hat{N}) \simeq \frac{\left( e^{\frac{4\hat{N}\xi}{3\xi+1}} \xi \left( e^{\frac{4\hat{N}\xi}{3\xi+1}} + \kappa^2 \xi \phi_e^2 - 1 \right) \right)^{\frac{1}{2}}}{e^{\frac{4\hat{N}\xi}{3\xi+1}} \xi \kappa}. \quad (66)$$

Finally, adopting the mentioned forms of the potential and the non-minimal coupling function results in the following expressions for the local non-linear parameters associated to both bispectrum and trispectrum of the model in Einstein frame

$$\frac{6}{5}\hat{f}_{NL}^{local} = \frac{(m_\phi^2\phi(1+\kappa^2\xi\phi^2) - 2\kappa^2m_\phi^2\phi^3\xi)^2}{\kappa^4m_\phi^4\phi^4} \left( -\frac{4\kappa^2m_\phi^2\phi(1+\kappa^2\xi\phi^2 + 6\kappa^2\xi^2\phi^2)}{(1+\kappa^2\xi\phi^2)(m_\phi^2\phi(1+\kappa^2\xi\phi^2) - 2\kappa^2m_\phi^2\phi^3\xi)} - \right. \quad (67)$$

$$\frac{2\kappa^2m_\phi^2\phi^2(2\kappa^2\xi\phi + 12\kappa^2\xi^2\phi)}{(1+\kappa^2\xi\phi^2)(m_\phi^2\phi(1+\kappa^2\xi\phi^2) - 2\kappa^2m_\phi^2\phi^3\xi)} + \frac{4\kappa^4m_\phi^2\phi^3(1+\kappa^2\xi\phi^2 + 6\kappa^2\xi^2\phi^2)\xi}{(1+\kappa^2\xi\phi^2)^2(m_\phi^2\phi(1+\kappa^2\xi\phi^2) - 2\kappa^2m_\phi^2\phi^3\xi)} +$$

$$\left. \frac{2\kappa^2m_\phi^2\phi^2(1+\kappa^2\xi\phi^2 + 6\kappa^2\xi^2\phi^2)(m_\phi^2(1+\kappa^2\xi\phi^2) - 4m_\phi^2\phi^2\kappa^2\xi)}{(1+\kappa^2\xi\phi^2)(m_\phi^2\phi(1+\kappa^2\xi\phi^2) - 2\kappa^2m_\phi^2\phi^3\xi)^2} \right) \frac{(1+\kappa^2\xi\phi^2)^2}{(1+\kappa^2\xi\phi^2 + 6\kappa^2\xi^2\phi^2)^2},$$

$$\hat{\tau}_{NL}^{local} = \frac{16(m_\phi^2\phi(1+\kappa^2\xi\phi^2) - 2\kappa^2m_\phi^2\phi^3\xi)^4}{\kappa^8m_\phi^8\phi^8} \left( -\frac{\kappa^2m_\phi^2\phi(1+\kappa^2\xi\phi^2 + 6\kappa^2\xi^2\phi^2)}{(1+\kappa^2\xi\phi^2)(m_\phi^2\phi(1+\kappa^2\xi\phi^2) - 2\kappa^2m_\phi^2\phi^3\xi)} - \right. \quad (68)$$

$$\frac{\kappa^2m_\phi^2\phi^2(2\kappa^2\xi\phi + 12\kappa^2\xi^2\phi)}{2(1+\kappa^2\xi\phi^2)(m_\phi^2\phi(1+\kappa^2\xi\phi^2) - 2\kappa^2m_\phi^2\phi^3\xi)} + \frac{\kappa^4m_\phi^2\phi^3(1+\kappa^2\xi\phi^2 + 6\kappa^2\xi^2\phi^2)\xi}{(1+\kappa^2\xi\phi^2)^2(m_\phi^2\phi(1+\kappa^2\xi\phi^2) - 2\kappa^2m_\phi^2\phi^3\xi)} +$$

$$\left. \frac{\kappa^2m_\phi^2\phi^2(1+\kappa^2\xi\phi^2 + 6\kappa^2\xi^2\phi^2)(m_\phi^2(1+\kappa^2\xi\phi^2) - 4m_\phi^2\phi^2\kappa^2\xi)}{2(1+\kappa^2\xi\phi^2)(m_\phi^2\phi(1+\kappa^2\xi\phi^2) - 2\kappa^2m_\phi^2\phi^3\xi)^2} \right)^2 \frac{(1+\kappa^2\xi\phi^2)^4}{(1+\kappa^2\xi\phi^2 + 6\kappa^2\xi^2\phi^2)^4},$$

and

$$\frac{54}{25}\hat{g}_{NL}^{local} = -\frac{8(m_\phi^2\phi(1+\kappa^2\xi\phi^2) - 2\kappa^2m_\phi^2\phi^3\xi)^2}{\kappa^6m_\phi^6\phi^6(1+\kappa^2\xi\phi^2)} \left( -\kappa^2m_\phi^2(1+\kappa^2\xi\phi^2 + 6\kappa^2\xi^2\phi^2) \right. \quad (69)$$

$$-2\kappa^2m_\phi^2\phi(2\kappa^2\xi\phi + 12\kappa^2\xi^2\phi) + 5\kappa^4m_\phi^2\phi^2(1+\kappa^2\xi\phi^2 + 6\kappa^2\xi^2\phi^2)\xi(1+\kappa^2\xi\phi^2)^{-1} +$$

$$\frac{2\kappa^2m_\phi^2\phi(1+\kappa^2\xi\phi^2 + 6\kappa^2\xi^2\phi^2)(m_\phi^2(1+\kappa^2\xi\phi^2) - 4m_\phi^2\phi^2\kappa^2\xi)}{(m_\phi^2\phi(1+\kappa^2\xi\phi^2) - 2\kappa^2m_\phi^2\phi^3\xi)} - \frac{1}{2}m_\phi^2\phi^2\kappa^2(2\kappa^2\xi + 12\kappa^2\xi^2) +$$

$$\frac{2\kappa^4m_\phi^2\phi^3(2\kappa^2\xi\phi + 12\kappa^2\xi^2\phi)\xi}{(1+\kappa^2\xi\phi^2)} + \frac{m_\phi^2\phi^2\kappa^2(2\kappa^2\xi\phi + 12\kappa^2\xi^2\phi)(m_\phi^2(1+\kappa^2\xi\phi^2) - 4m_\phi^2\phi^2\kappa^2\xi)}{(m_\phi^2\phi(1+\kappa^2\xi\phi^2) - 2\kappa^2m_\phi^2\phi^3\xi)} -$$

$$\frac{4\kappa^6m_\phi^2\phi^4(1+\kappa^2\xi\phi^2 + 6\kappa^2\xi^2\phi^2)\xi^2}{(1+\kappa^2\xi\phi^2)^2} - 3\frac{\kappa^4m_\phi^4\phi^3(1+\kappa^2\xi\phi^2 + 6\kappa^2\xi^2\phi^2)\xi}{(m_\phi^2\phi(1+\kappa^2\xi\phi^2) - 2\kappa^2m_\phi^2\phi^3\xi)} -$$

$$\frac{2\kappa^4m_\phi^2\phi^3(1+\kappa^2\xi\phi^2 + 6\kappa^2\xi^2\phi^2)\xi(m_\phi^2(1+\kappa^2\xi\phi^2) - 4m_\phi^2\phi^2\kappa^2\xi)}{(1+\kappa^2\xi\phi^2)(m_\phi^2\phi(1+\kappa^2\xi\phi^2) - 2\kappa^2m_\phi^2\phi^3\xi)} -$$

$$\left. \frac{m_\phi^2\phi^2\kappa^2(1+\kappa^2\xi\phi^2 + 6\kappa^2\xi^2\phi^2)(m_\phi^2(1+\kappa^2\xi\phi^2) - 4m_\phi^2\phi^2\kappa^2\xi)^2}{(m_\phi^2\phi(1+\kappa^2\xi\phi^2) - 2\kappa^2m_\phi^2\phi^3\xi)^2} \right) \frac{(1+\kappa^2\xi\phi^2)^3}{(1+\kappa^2\xi\phi^2 + 6\kappa^2\xi^2\phi^2)^3}.$$

Now we can substitute the field value in Einstein frame, that is, equation (66) in Eqs. (67), (68) and (69) to obtain the intended non-linear parameters as a function of  $N$ . In the next section we perform some numerical analysis on the model's parameter space in the Einstein. We study numerically  $\hat{f}_{NL}^{local}$ ,  $\hat{\tau}_{NL}^{local}$  and  $\hat{g}_{NL}^{local}$  to see the behaviors of these quantities in Einstein frame and compare the results with their Jordan frame's counterparts.

### VIII. CONFRONTATION WITH OBSERVATION

As for Jordan frame, we should firstly obtain the value of the inflaton field at the end of inflation,  $\phi_e$ . By studying the evolution of the slow-roll parameters, one can find the value of the inflaton field at the end of inflation (that

is, for  $\hat{\epsilon} \rightarrow 1$  or  $\hat{\eta} \rightarrow 1$ ). Using the definition of the slow-roll parameters in Einstein frame as  $\hat{\epsilon} = \frac{1}{2\kappa^2} \left( \frac{\dot{V}_{,\phi}}{V} \right)^2$  and  $\hat{\eta} = \frac{1}{\kappa^2} \left( \frac{\ddot{V}_{,\phi\phi}}{V} \right)$ , we obtain the following expressions

$$\hat{\epsilon} = \frac{1}{2\kappa^2} \frac{\left( V_{,\phi}(1+2\kappa^2f) - 4\kappa^2Vf_{,\phi} \right)^2}{V^2(1+2\kappa^2f+6\kappa^2f_{,\phi}^2)}, \quad (70)$$

and

$$\hat{\eta} = \frac{(1+2\kappa^2f)^2}{\kappa^2V} \frac{d^2}{d\hat{\phi}^2} \left( \frac{V}{(1+2\kappa^2f)^2} \right). \quad (71)$$

Fig. 10 shows the behavior of  $\hat{\epsilon}$  versus  $\hat{\phi}$  and  $\xi$ . It is obvious from this figure that the value of  $\hat{\phi}_e$  is directly dependant on the non-minimal coupling parameter. The

value of the field at the end of inflation in Einstein frame is given by the following expression

$$\hat{\phi}_e = \frac{\sqrt{\xi(4\xi+1)\left(-4\xi-1+\sqrt{48\xi^2+16\xi+1}\right)}}{\sqrt{2}\xi\kappa(4\xi+1)}. \quad (72)$$

After obtaining the field value at the end of inflation in Einstein frame, now we are in the position to study the non-Gaussianity of the model at hand through its non-linear parameters. Fig. 11 demonstrates the relation between  $\hat{f}_{NL}^{local}$  and parameters  $\xi$  and  $\hat{N}$  in Einstein frame. This figure confirms that for any value of  $\xi$ , the absolute value of  $\hat{f}_{NL}^{local}$  increases during the inflation era in this frame (similar to the Jordan frame case). This property is more clarified in the left panel of Fig. 12 which shows the behavior of this parameter in the number of e-folds space for various values of  $\xi$ . The right panel of Fig. 12 also shows the behavior in  $\xi$  space in Einstein frame about the end of inflation. As an important result we can see from the left panel of Fig. 12 that the first order non-Gaussian effect is almost constant and small at the initial stage of the inflationary era and then grows gradually to values of order unity at the time of horizon crossing (similar to the Jordan frame case). The behaviors of trispectrum non-linear parameters,  $\hat{\tau}_{NL}^{local}$  and  $\hat{g}_{NL}^{local}$  in  $\xi$  and  $\hat{N}$  spaces in Einstein frame are shown in Figs. 13 and 15. Moreover, the behavior of the trispectrum non-linear parameters versus  $\hat{N}$  are depicted in the left panels of Figs. 14 and 16. In order to see the effect of the non-minimal coupling parameter on the level of trispectrum in Einstein frame, the right panels of Figs. 14 and 16 have been plotted about the end of inflation. We note that while the overall behaviors of non-linear parameters in two frames are the same, the values of these parameters are not the same in two frames as usual. Specially, the value of the non-linear parameter  $\hat{g}_{NL}^{local}$  in Einstein frame is not as large as the  $\hat{g}_{NL}^{local}$  values in Jordan frame. This is reasonable since in Einstein frame one essentially deals with a minimally coupled redefined scalar field and it is natural to recover the standard results for a minimally coupled single scalar field as has been reported in [15]. Once again we emphasize that the larger values of  $\hat{g}_{NL}^{local}$  in Jordan frame in comparison with Einstein frame has its origin on the non-minimal coupling between the scalar field and curvature in Jordan frame.

After illustrating the behavior of bispectrum and trispectrum separately, now we are in the position to constrain the model in Einstein frame with observations. Similar to our numerical analysis in Jordan frame, we explore the behavior of  $\hat{f}_{NL}^{local}$  versus  $\hat{g}_{NL}^{local}$  with local configuration in the background of the Planck2015 data to see the viability of the inflation in Einstein frame in confrontation with the recent observations. This behavior is shown in Fig. 17. Similar to our result in Jordan frame, this figure confirms that although our non-Gaussian results in Einstein frame are somehow small, however they

are well inside the region allowed by the Planck observations. This figure confirms also that our model is consistent with observation for all values of  $\xi$ , that is  $0 < \xi \leq \frac{1}{6}$ , in Einstein frame. Furthermore, Fig. 18 shows the amplitude of  $\hat{\tau}_{NL}^{local}$  versus  $\hat{g}_{NL}^{local}$  for local configuration of non-Gaussianity in Einstein frame with quadratic functions for  $V(\phi)$  and  $f(\phi)$  in the background of Planck2013 data. It is again clear that a non-minimal inflation in Einstein frame is consistent with observation for all values of  $\xi$ . We note that the results obtained in this case are compatible with the results obtained for  $\hat{f}_{NL}^{local}$  versus  $\hat{g}_{NL}^{local}$ . Moreover, comparing these results, which are obtained in Einstein frame, with previous results obtained in Jordan frame overall confirms that both cases match together as well.

## IX. SUMMARY AND CONCLUSION

In this paper we have studied the dynamics of an inflationary model driven by a scalar field that is coupled non-minimally with gravity. At first, we have obtained the main equations of the model. Then, imposing slow-roll approximation, we have studied bispectrum and trispectrum of the curvature perturbations. We focused on the local shape of non-Gaussianity which has a peak at the squeezed limit (where two wave numbers are much larger than the third one,  $k_1 = k_2 \gg k_3$ ). This shape of non-Gaussianity illustrates large super-Hubble interactions. On super-horizon scales we can only use the evolution of unperturbed separate universes and neglect spatial gradients. To proceed further, we applied a formalism which provides a powerful tool in evaluating the evolution of the curvature perturbation on this scales, the so-called  $\delta N$  formalism. The main advantage of this approach is that allows the primordial curvature perturbation to be related to the difference of  $N$  between the perturbed universe and the homogeneous background one. We calculated these values between an initially flat hypersurface (with  $t_*$  corresponding to the time of horizon crossing) and a final uniform energy density hypersurface (with  $t_e$  referring to the end of inflation) for the model at hand. By choosing the flat slicing gauge and considering perturbations, we have expanded the inflaton field around a homogeneous background and local perturbation and found  $\zeta$  as an expansion of  $\delta\phi$ . Then we have employed the  $\delta N$  expansion and used the two-point correlation function to find the dimensionless power spectrum in terms of the derivatives of  $N$  with respect to the inflaton field. In order to obtain the lowest order of non-Gaussianity, the bispectrum  $B_\zeta$ , we applied the three-point correlation function. Since in this work we have been interested in local non-Gaussianities, which are confirmed on super-horizon scales, we only need the momentum independent term of the bispectrum that accounts for the super-horizon contribution. Next we have obtained the non-linear parameter associated to the first order of local non-Gaussianity,  $f_{NL}^{local}$ , in terms of  $N_{,\phi}$  and

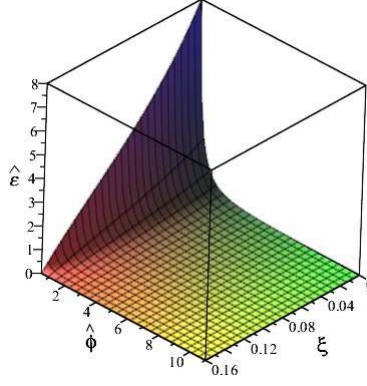


FIG. 10. The behavior of  $\hat{\epsilon}$  versus  $\hat{\phi}$  and  $\xi$  for non-minimal inflation in Einstein frame.

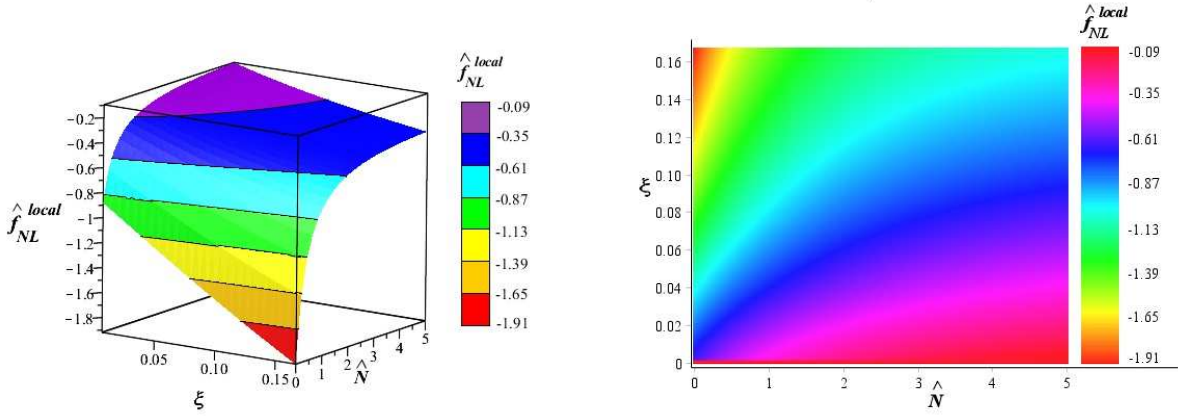


FIG. 11. The non-linear parameter  $\hat{f}_{NL}^{local}$  as a function of the non-minimal coupling parameter  $\xi$  and the number of e-folds  $\hat{N}$  for non-minimal inflation in Einstein frame.

$N_{,\phi\phi}$ . Furthermore, to describe the four-point correlation function, or the trispectrum, using  $\delta N$  formalism, we have obtained the relevant non-linear parameters,  $\tau_{NL}^{local}$  and  $g_{NL}^{local}$ . Although  $\tau_{NL}^{local}$  depends only on the first and second derivatives of  $N$  (which makes it capable to be expressed in terms of  $f_{NL}^{local}$ ),  $g_{NL}^{local}$  depends on the third order of this derivative,  $N_{,\phi\phi\phi}$  too. After explaining the numerical method for calculating derivatives of the unperturbed number of e-folds with respect to the unperturbed inflaton field at horizon crossing and showing how these derivatives are related to the field description, we obtained the exact form of parameters in terms of  $\xi$  and  $\phi$ . After deriving the mentioned non-linear parameters as a product of  $N$ 's derivatives, we have studied their evolution. To this end, we have first adopted a quadratic form for both potential and non-minimal coupling function as  $V(\phi) = \frac{1}{2}m_\phi^2\phi^2$  and  $f(\phi) = \frac{1}{2}\xi\phi^2$ . Finally, after obtaining the field's value during slow-roll inflation in terms of the number of e-folds, we were able to depict the evolution of the non-linear parameters in  $\xi$  and  $N$  space. One can see Fig. 2- 7 to follow how  $f_{NL}^{local}$ ,  $\tau_{NL}^{local}$  and  $g_{NL}^{local}$  evolve in  $N$  and  $\xi$  space, both simultaneously

and separately.

Eventually we have explored the behavior of the  $f_{NL}^{local}$  versus  $g_{NL}^{local}$  with local configuration in the background of the Planck2015 data to see the viability of this theoretical model. Our analysis confirms that for all chosen values of  $\xi$  the model is consistent with observation. We have also studied the behavior of  $g_{NL}^{local}$  versus  $\tau_{NL}^{local}$  using the results of [33]. Our result in this case is also consistent with observation for all values of the non-minimal coupling parameter,  $\xi$ .

As an important achievement of this study, although we haven't obtained large local non-Gaussianities of perturbations in this non-minimal setup, however it is in well agreement with Planck observations. Since there is no observational difference in between Jordan and Einstein frames at least in the single field case, we have moved to Einstein frame to see the situation in this frame. We have checked the consistency conditions in this frame. The non-Gaussianities are small in this frame too.

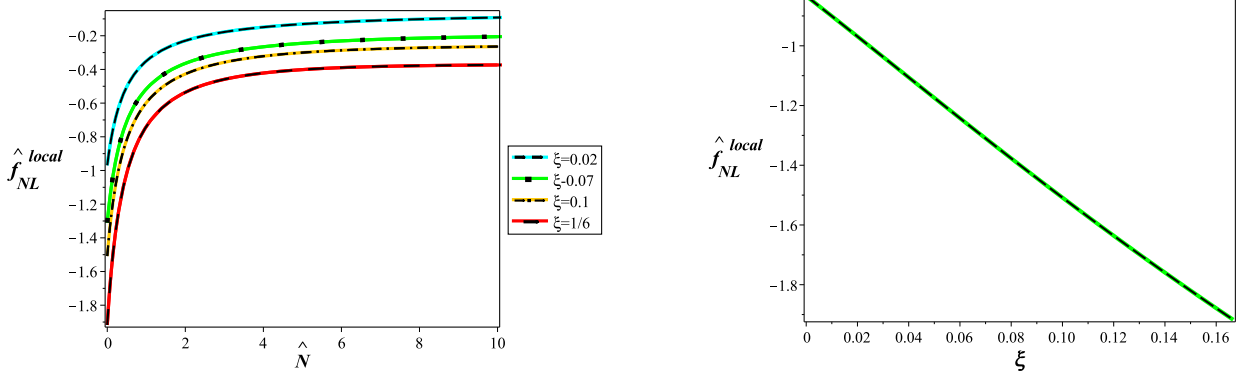


FIG. 12. Left Panel: The non-linear parameter  $\hat{f}_{NL}^{local}$  for the local type non-Gaussianity versus the number of e-folds for various values of the non-minimal coupling parameter in Einstein frame. Right Panel: The non-linear parameter  $\hat{f}_{NL}^{local}$  for the local type non-Gaussianity as a function of the non-minimal coupling parameter in Einstein frame about the time that cosmological scales exit the Hubble horizon.

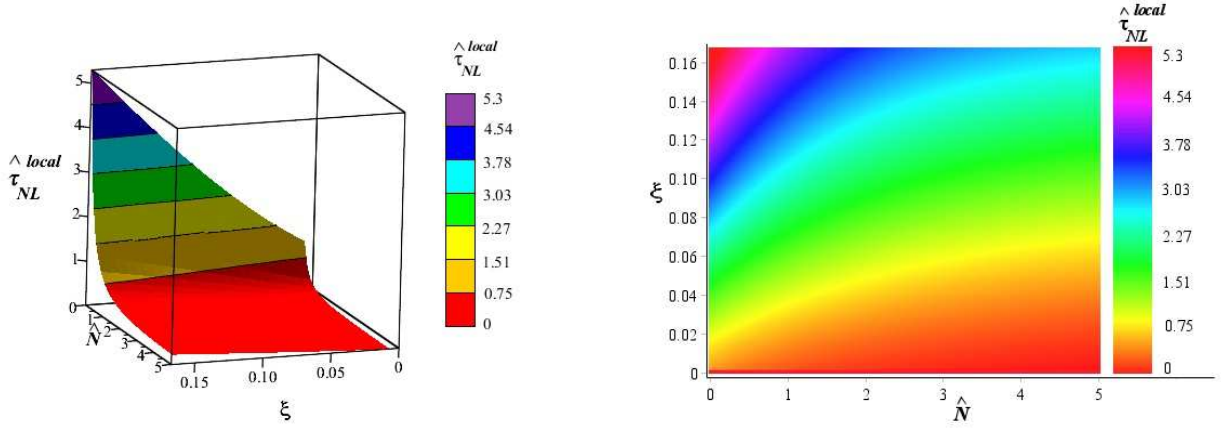


FIG. 13. The non-linear parameter  $\hat{\tau}_{NL}^{local}$  as a function of the non-minimal coupling parameter  $\xi$  and the number of e-folds  $\hat{N}$  for non-minimal inflation in Einstein frame.

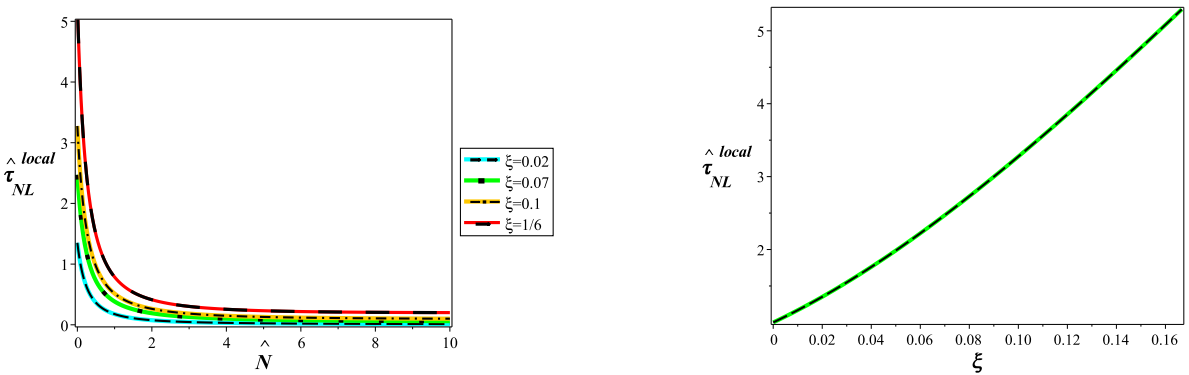


FIG. 14. Left Panel: The non-linear parameter  $\hat{\tau}_{NL}^{local}$  for the local type non-Gaussianity versus the number of e-folds for various values of the non-minimal coupling parameter for non-minimal inflation in Einstein frame. Right Panel: The non-linear parameter  $\hat{\tau}_{NL}^{local}$  for the local type non-Gaussianity as a function of the non-minimal coupling parameter about the time that cosmological scales exit the Hubble horizon for non-minimal inflation in Einstein frame.

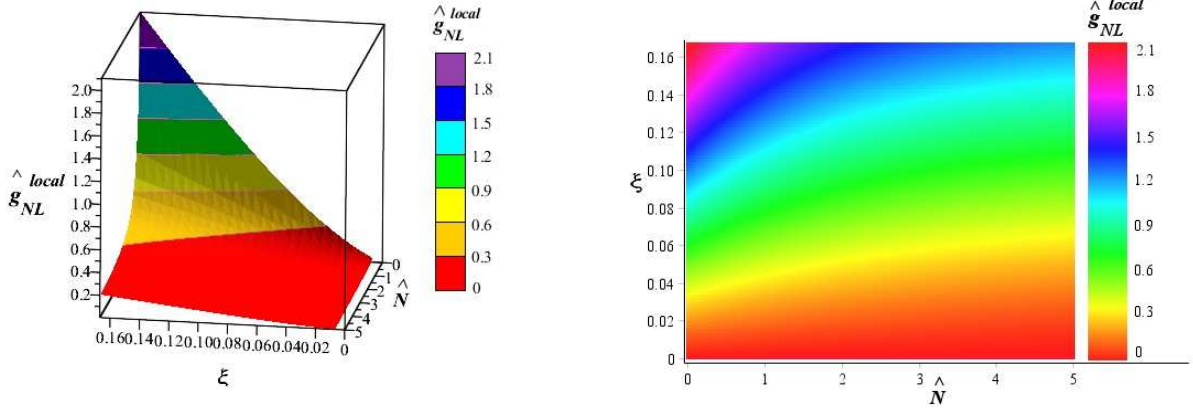


FIG. 15. The non-linear parameter  $\hat{g}_{NL}^{local}$  as a function of the non-minimal coupling parameter  $\xi$  and the number of e-folds  $\hat{N}$  for non-minimal inflation in Einstein frame.

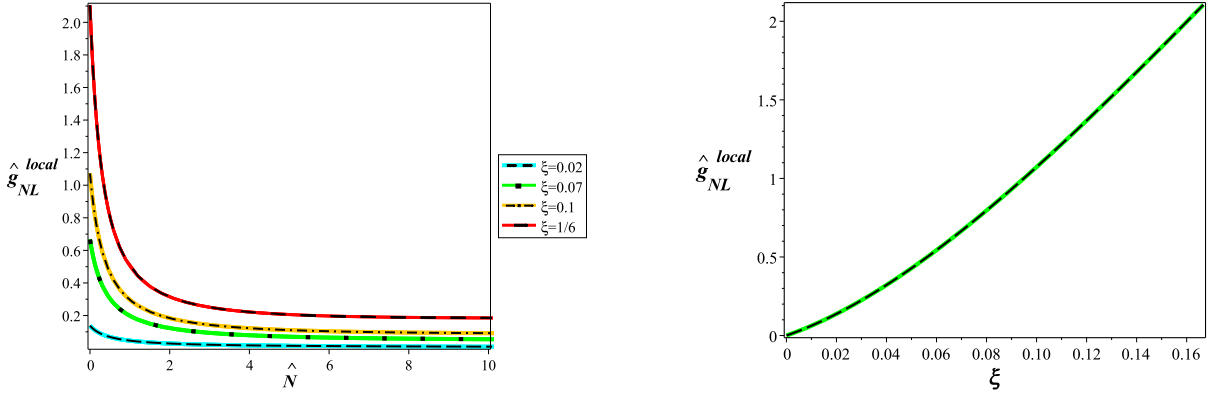


FIG. 16. Left Panel: The non-linear parameter  $\hat{g}_{NL}^{local}$  for the local type non-Gaussianity versus the number of e-folds for various values of the non-minimal coupling parameter for non-minimal inflation in Einstein frame. Right panel: The non-linear parameter  $\hat{g}_{NL}^{local}$  for the local type non-Gaussianity as a function of the non-minimal coupling parameter about the time that cosmological scales exit the Hubble horizon for non-minimal inflation in Einstein frame.

### Appendix A: Derivatives of the number of e-folds with respect to the scalar field in Einstein frame

number of e-folds take the following forms

$$\hat{N}_{,\phi} = -\kappa^2 \frac{V \left[ (1 + 2\kappa^2 f) + 6\kappa^2 f_{,\phi}^2 \right]}{(1 + 2\kappa^2 f) [V_{,\phi} (1 + 2\kappa^2 f) - 4\kappa^2 V f_{,\phi}]}, \quad (73)$$

Using Eq. (63), the first and second derivatives of the

and

$$\begin{aligned} \hat{N}_{,\phi\phi} = & -\kappa^2 \frac{V_{,\phi} \left[ (1 + 2\kappa^2 f) + 6\kappa^2 f_{,\phi}^2 \right]}{(1 + 2\kappa^2 f) [V_{,\phi} (1 + 2\kappa^2 f) - 4\kappa^2 V f_{,\phi}]} - \kappa^2 \frac{V [2\kappa^2 f_{,\phi} + 12\kappa^2 f_{,\phi} f_{,\phi\phi}]}{(1 + 2\kappa^2 f) [V_{,\phi} (1 + 2\kappa^2 f) - 4\kappa^2 V f_{,\phi}]} \\ & + \kappa^2 \frac{V \left[ (1 + 2\kappa^2 f) + 6\kappa^2 f_{,\phi}^2 \right] [V_{,\phi\phi} (1 + 2\kappa^2 f) + 2\kappa^2 V_{,\phi} f_{,\phi} - 4\kappa^2 V_{,\phi} f_{,\phi\phi} - 4\kappa^2 V f_{,\phi\phi}]}{(1 + 2\kappa^2 f) [V_{,\phi} (1 + 2\kappa^2 f) - 4\kappa^2 V f_{,\phi}]^2} \\ & + \kappa^2 \frac{2\kappa^2 V f_{,\phi} \left[ (1 + 2\kappa^2 f) + 6\kappa^2 f_{,\phi}^2 \right]}{(1 + 2\kappa^2 f)^2 [V_{,\phi} (1 + 2\kappa^2 f) - 4\kappa^2 V f_{,\phi}]}, \end{aligned} \quad (74)$$

respectively. Also, the third derivative of  $N$  gives the following expression

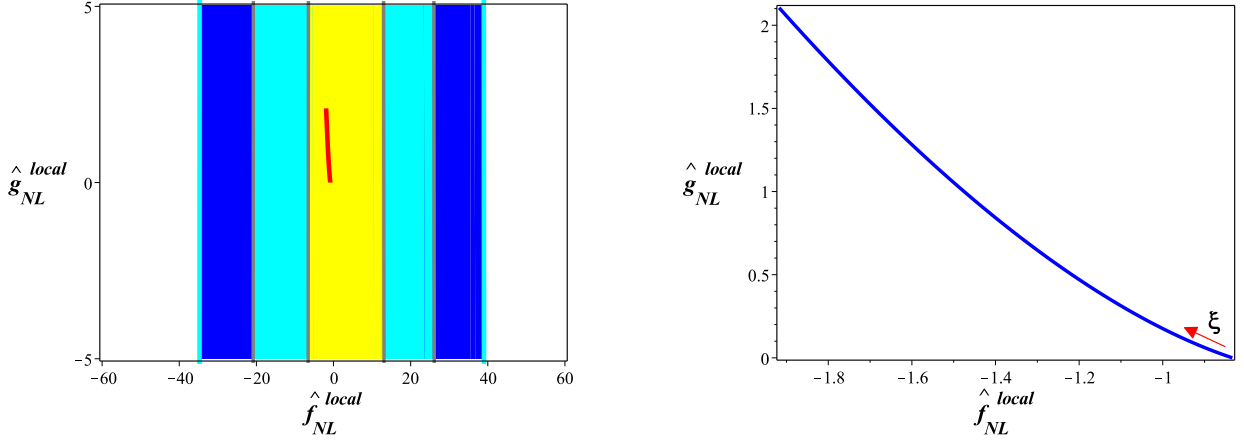


FIG. 17. The amplitude of  $\hat{g}_{NL}^{local}$  versus  $\hat{f}_{NL}^{local}$  for local configuration of non-Gaussianity in Einstein frame in the background of Planck2015 data. These figures are plotted about the end of inflation for a quadratic potential and the non-minimal coupling function as  $f(\phi) \sim \xi\phi^2$ . We note that the red line in this figure shows the position of our result in the background of the observational data. The right panel highlights more details of  $\hat{g}_{NL}^{local}$  versus  $\hat{f}_{NL}^{local}$  in terms of  $\xi$ .

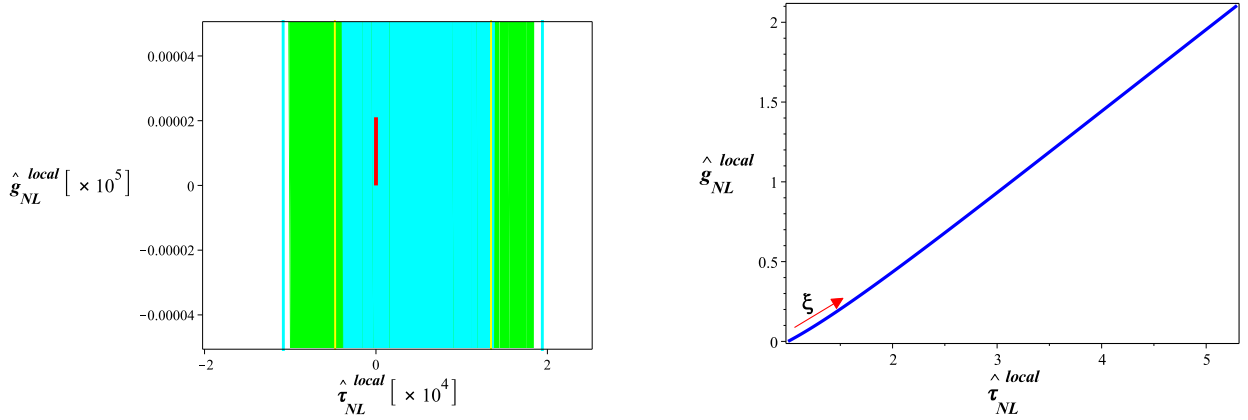


FIG. 18. The amplitude of  $\hat{g}_{NL}^{local}$  versus  $\hat{\tau}_{NL}^{local}$  for local configuration of non-Gaussianity in Einstein frame in the background of Planck2013 data. These figures are plotted about the end of inflation for a quadratic potential and the non-minimal coupling function as  $f(\phi) \sim \xi\phi^2$ . We note that the red line in this figure shows the position of our result in the background of the observational data. The right panel highlights more details of  $\hat{g}_{NL}^{local}$  versus  $\hat{\tau}_{NL}^{local}$  in terms of  $\xi$ .

$$\begin{aligned}
\hat{N}_{,\phi\phi\phi} = & \left\{ -\kappa^2 V_{,\phi\phi} [(1+2\kappa^2 f) + 6\kappa^2 f_{,\phi}^2] - 2\kappa^2 V_{,\phi} [2\kappa^2 f_{,\phi} + 12\kappa^2 f_{,\phi} f_{,\phi\phi}] - \right. \\
& \kappa^2 V [2\kappa^2 f_{,\phi\phi} + 12\kappa^2 f_{,\phi\phi}^2 + 12\kappa^2 f_{,\phi} f_{,\phi\phi\phi}] + [1+2\kappa^2 f]^{-1} \left[ 2\kappa^4 f_{,\phi} V_{,\phi} [(1+2\kappa^2 f) + 6\kappa^2 f_{,\phi}^2] + \right. \\
& \left. 2\kappa^4 V f_{,\phi\phi} [(1+2\kappa^2 f) + 6\kappa^2 f_{,\phi}^2] + 2\kappa^4 V f_{,\phi} [2\kappa^2 f_{,\phi} + 12\kappa^2 f_{,\phi} f_{,\phi\phi}] \right] - 4\kappa^6 V f_{,\phi}^2 (1+2\kappa^2 f)^{-2} \times \\
& [(1+2\kappa^2 f) + 6\kappa^2 f_{,\phi}^2] + \left[ \kappa^2 V_{,\phi} [(1+2\kappa^2 f) + 6\kappa^2 f_{,\phi}^2] [V_{,\phi\phi}(1+2\kappa^2 f) - 2V_{,\phi}\kappa^2 f_{,\phi} - 4\kappa^2 V f_{,\phi\phi}] + \right. \\
& \left. \kappa^2 V [2\kappa^2 f_{,\phi} + 12\kappa^2 f_{,\phi} f_{,\phi\phi}] [V_{,\phi\phi}(1+2\kappa^2 f) + 2\kappa^2 V_{,\phi} f_{,\phi} - 4\kappa^2 V_{,\phi} f_{,\phi} - 4\kappa^2 V f_{,\phi\phi}] + \right. \\
& \left. \kappa^2 V [(1+2\kappa^2 f) + 6\kappa^2 f_{,\phi}^2] [V_{,\phi\phi\phi}(1+2\kappa^2 f) - 6\kappa^2 V_{,\phi} f_{,\phi\phi} - 4\kappa^2 V f_{,\phi\phi\phi}] \right] \times \\
& \left[ V_{,\phi}(1+2\kappa^2 f) - 4\kappa^2 V f_{,\phi} \right]^{-1} - \kappa^2 V [(1+2\kappa^2 f) + 6\kappa^2 f_{,\phi}^2] [V_{,\phi}(1+2\kappa^2 f) - 4\kappa^2 V f_{,\phi}]^{-2} \times \\
& \left. [V_{,\phi\phi}(1+2\kappa^2 f) + 2V_{,\phi}\kappa^2 f_{,\phi} - 4\kappa^2 V_{,\phi} f_{,\phi} - 4\kappa^2 V f_{,\phi\phi}]^2 \right\} \left[ (1+2\kappa^2 f) [V_{,\phi}(1+2\kappa^2 f) - \right. \\
& \left. 4\kappa^2 V f_{,\phi}] \right]^{-1} + \left\{ \kappa^2 V_{,\phi} [(1+2\kappa^2 f) + 6\kappa^2 f_{,\phi}^2] + \kappa^2 V [2\kappa^2 f_{,\phi} + 12\kappa^2 f_{,\phi} f_{,\phi\phi}] - 2\kappa^2 f_{,\phi} (1+2\kappa^2 f)^{-1} \right. \\
& \left. [\kappa^2 V(1+2\kappa^2 f) + 6\kappa^2 f_{,\phi}^2] - \kappa^2 V [V_{,\phi\phi}(1+2\kappa^2 f) + 2V_{,\phi}\kappa^2 f_{,\phi} - 4\kappa^2 V_{,\phi} f_{,\phi} - 4\kappa^2 V f_{,\phi\phi}] \times \right. \\
& \left. [(1+2\kappa^2 f) + 6\kappa^2 f_{,\phi}^2] [V_{,\phi}(1+2\kappa^2 f) - 4\kappa^2 V f_{,\phi}]^{-1} \right\} A \left[ (1+2\kappa^2 f) [V_{,\phi}(1+2\kappa^2 f) - 4\kappa^2 V f_{,\phi}] \right]^{-2},
\end{aligned} \tag{75}$$

where

$$\begin{aligned}
A = & (1+2\kappa^2 f) \left[ V_{,\phi\phi}(1+2\kappa^2 f) - 2\kappa^2 V_{,\phi} f_{,\phi} - 4\kappa^2 V_{,\phi} f_{,\phi\phi} \right] + \\
& 2\kappa^2 f_{,\phi} [V_{,\phi}(1+2\kappa^2 f) - 4\kappa^2 V f_{,\phi}].
\end{aligned} \tag{76}$$

---

**Appendix B: The first, second and third non-linear parameters for the local configuration in Einstein frame**

$$\begin{aligned}
\frac{6}{5} \hat{f}_{NL}^{local} = & -\frac{1}{\kappa^2} \frac{V_{,\phi}(1+2\kappa^2 f) [V_{,\phi}(1+2\kappa^2 f) - 4\kappa^2 V f_{,\phi}]}{V^2 [(1+2\kappa^2 f) + 6\kappa^2 f_{,\phi}^2]} - \\
& \frac{1}{\kappa^2} \frac{[2\kappa^2 f_{,\phi} + 12\kappa^2 f_{,\phi} f_{,\phi\phi}] (1+2\kappa^2 f) [V_{,\phi}(1+2\kappa^2 f) - 4\kappa^2 V f_{,\phi}]}{V [(1+2\kappa^2 f) + 6\kappa^2 f_{,\phi}^2]^2} + \\
& \frac{1}{\kappa^2} \frac{(1+2\kappa^2 f) [V_{,\phi\phi}(1+2\kappa^2 f) + 2\kappa^2 V_{,\phi} f_{,\phi} - 4\kappa^2 V_{,\phi} f_{,\phi} - 4\kappa^2 V f_{,\phi\phi}]}{V [(1+2\kappa^2 f) + 6\kappa^2 f_{,\phi}^2]} + \frac{1}{\kappa^2} \frac{2\kappa^2 f_{,\phi} [V_{,\phi}(1+2\kappa^2 f) - 4\kappa^2 V f_{,\phi}]}{V [(1+2\kappa^2 f) + 6\kappa^2 f_{,\phi}^2]}.
\end{aligned} \tag{77}$$



- [7] Barnaby, N., & Cline, J. M. 2006, *Phys. Rev. D* **73**, 106012 [arXiv:astro-ph/0601481].
- [8] Bartolo, N., Komatsu, E., Matarrese, S., & Riotto, A. 2004, *Phys. Rept.* **402**, 103 [arXiv:astro-ph/0406398].
- [9] Bartolo, N., Matarrese, S., & Riotto, A. 2004, *Phys. Rev. Lett.* **93**, 231301.
- [10] Bartolo, N., Matarrese, S., & Riotto, A. 2005, *J. Cosmol. Astropart. Phys.* **0508**, 010.
- [11] Bartolo, N., Fasiello, M., Matarrese, S., & Riotto, A. 2010, *J. Cosmol. Astropart. Phys.* 1008 008.
- [12] Bartolo, N., Fasiello, M., Matarrese, S., & Riotto, A. 2010, *J. Cosmol. Astropart. Phys.* 1009 035.
- [13] Bassett, B., Tsujikawa, S., & Wands, D. 2006, *Rev. Mod. Phys.* **78**, 537.
- [14] Bernardeau, F., & Uzan, J. P. 2003, *Phys. Rev. D* **67**, 121301 [arXiv:astro-ph/0209330].
- [15] Byrnes, C. T., Sasaki, M., & Wands, D. 2006, *Phys. Rev. D* **74**, 123519.
- [16] Byrnes, C. T., Koyama, K., Sasaki, M., & Wands, D. 2007, *J. Cosmol. Astropart. Phys.* **0711**, 027.
- [17] Byrnes, C. T., Choi, K. Y., & Hall, L. M. H. 2008, *J. Cosmol. Astropart. Phys.* **0810**, 008.
- [18] Byrnes C. T. & Tasinato, G. 2009, *J. Cosmol. Astropart. Phys.* **0908**, 016.
- [19] Byrnes, C. T., & Choi, K. Y. 2010, [arXiv:1002.3110].
- [20] Calzetta, E., & Hu, B. L. 1995, *Phys. Rev. D* **52**, 6770.
- [21] Chambers A. & Rajantie, A. 2008, *Phys. Rev. Lett.* **100**, 041302 [Erratum-ibid. 101, 149903].
- [22] Chambers, A., & Rajantie, A. 2008, *J. Cosmol. Astropart. Phys.* **0808**, 002.
- [23] Chen, X., Huang, M. -x., Kachru, S., & Shiu, G. 2007, *J. Cosmol. Astropart. Phys.* **0701**, 002.
- [24] Chen, X., & Wang, Y. 2010, *Phys. Rev. D* **81**, 063511.
- [25] Chen, X., & Wang, Y. 2010, *J. Cosmol. Astropart. Phys.* **1004**, 027.
- [26] Cogollo, H.R.S., Rodriguez, Y., & Valenzuela-Toledo, C.A. 2008, *J. Cosmol. Astropart. Phys.* **0808**, 029.
- [27] Creminelli, P. 2003, *J. Cosmol. Astropart. Phys.* **0310**, 003 [arXiv:astro-ph/0306122].
- [28] Creminelli, P., Nicolis, A., Senatore, L., Tegmark, M., & Zaldarriaga, M. 2006, *J. Cosmol. Astropart. Phys.* **0605**, 004.
- [29] Desjacques, V., & Seljak, U. 2010, *Phys. Rev., D* **81**, 023006.
- [30] Dodelson, S. 2008, Academic Press.
- [31] Dvali, G., Gruzinov A., & Zaldarriaga, M. 2004, *Phys. Rev. D* **69**, 023505 [arXiv:astro-ph/0303591].
- [32] Enqvist, K., Jokinen, A., Mazumdar, A., Multamaki, T., & Vaihkonen, A. 2005, *Phys. Rev. Lett.* **94**, 161301 [arXiv:astro-ph/0411394].
- [33] Feng, C., Cooray, A., Smidt, J., O'Bryan, J., Keating, B., & Regan, D. 2015, [arXiv:1502.00585].
- [34] Fergusson, J. R., Regan D. M., & Shellard, E. P. S. 2010b, ArXiv e-prints, [arXiv:1012.6039].
- [35] Ferreira, P., Magueijo, J., & Gorski, K. 1998, *Astrophys. J. Lett.* **503**, L1.
- [36] Gangui, A., Luchin, F., Matarrese, S., & Mollerach, S. 1994, *Astrophys. J.* **430**, 447.
- [37] Giannantonio, T., & Ross, A. J. 2014, *Phys. Rev., D* **89**, 023511.
- [38] Guth, A. 1981, *Phys. Rev. D* **23** 347.
- [39] Heavens, A. F. 1998, *Mon. Not. R. Astron. Soc.* **299**, 805.
- [40] Hikage, C., & Matsubara, T. 2012, *MNRAS*, **425**, 2187.
- [41] Hu, W. 2001, *Phys. Rev. D* **64**, 083005.
- [42] Jokinen, A., & Mazumdar, A. 2006, *J. Cosmol. Astropart. Phys.* **0604**, 003 [arXiv:astro-ph/0512368].
- [43] Kaiser, D. I. 2010, *Phys. Rev. D* **81**, 084044 [arXiv:1003.1159 [gr-qc]].
- [44] Kaiser, D. I., Mazenc, E. A. and Sfakianakis, E. I. 2013, *Physical Review D* **87** 064004.
- [45] Kenton, Z., & Mulryne, D. J. 2015, *J. Cosmol. Astropart. Phys.* **1510**, 018.
- [46] Kenton, Z., & Mulryne, D. J. 2016, [arXiv:1605.03435[astro-ph]].
- [47] Kogo, N., & Komatsu, E. 2006, *Phys. Rev. D* **73**, 083007.
- [48] Komatsu, E. et al. 2010, [arXiv:1001.4538].
- [49] Komatsu, E., & Spergel, D. N. 2001, *Phys. Rev. D* **63**, 063002 [arXiv:astro-ph/0005036].
- [50] Koyama, K. 2010, [arXiv:1002.0600].
- [51] Langlois, D., Maartens R. and Wands, D. 2000, *Phys. Lett. B*, **489**, 259.
- [52] Leistedt, B., Peiris H. V., & Roth, N. 2015, *Phys. Rev. Lett.* **113**, 221301.
- [53] Liddle, A., & Lyth, D. 2000, Cambridge University Press.
- [54] Lidsey, J. E., Liddle, A. R., Kolb, E.W., Copeland, E. J., Barreiro, T., & Abney, M. 1997, *Rev. Mod. Phys.* **69**, 373.
- [55] Linde, A. D. 1982, *Phys. Lett. B* **108** 389.
- [56] Linde, A. D. 1990, Harwood Academic Publishers, Chur, Switzerland, [arXiv:hep-th/0503203].
- [57] Lyth, D. H., Malik, K. A., & Sasaki, M. 2005, *J. Cosmol. Astropart. Phys.* **0505**, 004 [arXiv:astro-ph/0411220].
- [58] Lyth, D. H. 2005, *J. Cosmol. Astropart. Phys.* **0511**, 006 [arXiv:astro-ph/0510443].
- [59] Lyth, D. H., & Liddle, A. R. 2009, Cambridge University Press, Cambridge, England.
- [60] Lyth D. H., & Rodriguez, Y. 2005, *Phys. Rev. Lett.* **95**, 121302 [arXiv:astro-ph/0504045].
- [61] Lyth, D. H., & Zaballa, I. 2005, *J. Cosmol. Astropart. Phys.* **10**, 005.
- [62] Maldacena, J. M., *JHEP* **0305**, 013 [arXiv:astro-ph/0210603].
- [63] Malik, K. A., & Lyth, D. H. 2006, *J. Cosmol. Astropart. Phys.* **0609**, 008 [arXiv:astro-ph/0604387].
- [64] Malik, K. A., & Wands, D. 2004, *Class. Quant. Grav.* **21**, L65 [arXiv:astro-ph/0307055].
- [65] Mukhanov, V. F., Feldman, H. A., & Brandenberger, R. H. 1992, *Phys. Rept.* **215**, 203, Part 2.
- [66] Mulryne, D., Seery, D., & Wesley, D. 2009, [arXiv:0911.3550].
- [67] Nozari, K., & Asadi, K. 2016, *Phys. Rev. D* **350** 339.
- [68] Nozari, K., & Rashidi, N. 2012, *Phys. Rev. D* **86** (2012) 043505.
- [69] Nozari, K., & Rashidi, N. 2013, *Phys. Rev. D* **88** (2013) 023519.
- [70] Nozari, K., & Rashidi, N. 2013, *Phys. Rev. D* **88** 084040.
- [71] Nozari, K., & Rashidi, N. 2014, *Astrophys. Space Sci.* **350** 339.
- [72] Nozari, K., & Rashidi, N. 2016, *Phys. Rev. D* **93** 124022.
- [73] Nozari, K., & Rashidi, N. 2016, *Advances in High Energy Physics*, **2016**, 1252689 [arXiv:1509.06240].
- [74] Okamoto, T., & Hu, W. 2002, *Phys. Rev. D* **66**, 063008.
- [75] Regan, D., Gosenca, M., & Seery, D. 2013, [arXiv:1310.8617].
- [76] Rigopoulos, G., & Shellard, E. 2003, *Phys. Rev. D* **68**, 123518.
- [77] Riotto, A. 2002, [arXiv:hep-ph/0210162].
- [78] Rodriguez, Y., & Valenzuela-Toledo, C. A. 2010, *Phys.*

- Rev. D **81**, 023531.
- [79] Salem, M. P. 2005 Phys. Rev. D **72**, 123516 [arXiv:astro-ph/0511146].
- [80] Sasaki, M., Valiviita, J., & Wands, D. 2006, Phys. Rev. D **74**, 103003.
- [81] Sasaki, M., & Stewart, E. D. 1996, Prog. Theor. Phys. **95**, 71.
- [82] Sasaki, M., & Tanaka, T. 1998, Prog. Theor. Phys. **99**, 763.
- [83] Seery, D., Lidsey, J. E., & Sloth, M. S. 2007, J. Cosmol. Astropart. Phys. **0701**, 027 (2007).
- [84] Seery, D., & Lidsey, J. E. 2007, J. Cosmol. Astropart. Phys. **0701**, 008.
- [85] Sekiguchi, T., & Sugiyama, N., J. 2013, Cosmol. Astropart. Phys., **1309**, 002.
- [86] Smidt, J., Amblard, A., Byrnes, C. T., et al., 2010, Phys. Rev. D, **81**, 123007.
- [87] Smith, K. M., Senatore, L., & Zaldarriaga, M. 2015, [arXiv:1502.00635].
- [88] Starobinsky, A. A. 1985, Soviet Journal of Experimental and Theoretical Physics Letters **42**, 152.
- [89] Tanaka, T., Suyama, T., & Yokoyama, S. 2010, Class. Quant. Grav. **27**, 124003.
- [90] Verde, L., Wang, L. M., Heavens, A., & Kamionkowski, M. 2000, Mon. Not. Roy. Astron. Soc. **313**, L141.
- [91] Vernizzi, F., & Wands, D. 2006, J. Cosmol. Astropart. Phys. **0605**, 019.
- [92] Vielva, P. & Sanz, J. 2010, Mon. Not. Roy. Astron. Soc., **404**, 895.
- [93] Wands, D., Malik, K. A., Lyth, D. H., & Liddle, A. R. 2000, Phys. Rev. D **62**, 043527.
- [94] Wang, L. M., & Kamionkowski, M. 2000, Phys. Rev. D **61**, 063504.
- [95] Weinberg, S. 2008, Oxford University Press, Oxford, 9 England.
- [96] White, J., Minamitsuji, M. and Sasaki, M. 2013, JCAP **09** 015.
- [97] Yokoyama, S., Suyama, T., & Tanaka, T. 2008, Phys. Rev. D **77**, 083511.

